Winter 12-2023

Synthesis and characterization of colorimetric and flurometric chemosensor for trivalent metal Ions

Fazila Haque
fhaque@mail.stmarytx.edu

SYNTHESIS AND CHARACTERIZATION OF COLORIMETRIC AND FLUOROMETRIC CHEMOSENSOR FOR TRIVALENT METAL IONS

By:

Fazila Haque

HONORS THESIS

Presented in Partial Fulfillment Requirements for

Graduation from the Honors Program of

St. Mary's University

San Antonio, Texas

Approved by:

Dr. Susan Oxley

Thesis Supervisor

Dr. Camille Langston

Honors Program Director

December 6, 2023

Abstract

By

Fazila Haque

There are many biological and environmental uses for trivalent metals (like Fe^{3+}, Al^{3+}, and Cr^{3+}) within our daily lives. Whether these trivalent metals are found in deficiency or excess can cause issues within our environment (global warming) or our bodies (can cause problems with our digestive, cardiovascular, and immune systems). Being able to detect them and understanding their importance becomes crucial in our understanding of the world that surrounds us.

One of the ways we can detect these trivalent metals is through the use of chemosensors. Chemosensors are used to sense analyte (trivalent metal) to produce a signal (fluorescence or absorbance). Much research has been done about trivalent colorimetric and fluorometric chemosensors, but many of these have complex syntheses to obtain the primary ligand used for trivalent metal detection, and even with such complex ligands the detection limit is still unreasonably high.

A chemosensor that is selective and sensitive to the trivalent metals (Al^{3+}, Fe^{3+}, and Cr^{3+}) while aiming for a low detection limit and a simple synthesis for the ligand would save time and resources needed for trivalent chemosensors. This colorimetric and fluorometric chemosensor is proven useful in environmental applications, provides aid in research regarding the impacts of these metals in the environment, and the medical field, helpful for diagnostics and imaging, will allow for advancements in both fields. This researched successfully obtained a chemosensor with a low limit of detection, ranging from 0.067-0.092μM for absorbance and 0.016-0.019μM for fluorescence.

This thesis is dedicated to Dr. Oxley, all my other professors, friends, and family that have helped and supported me throughout my academic/ professional career.

Table of Contents

FIGURES

TABLES

ACKNOWLEDGMENTS

My academic journey throughout the years has allowed me to meet brilliant individuals, and has provided a multitude of skills and knowledge that have given me insight into the world of science as a student. I would like to extend my gratitude to Dr. Susan Oxley who has provided me with such amazing guidance, from data collection to writing my thesis, as a mentor throughout this entire process. I would also like to thank my other professors and advisors throughout the years as they have guided me into preparing for my future career. Lastly, this entire project would not have been possible without the funding and support of the Welch Foundation (Grant U-0047) and St. Mary's University Chemistry/ Biochemistry Department.

CHAPTER 1: INTRODUCTION

There are many biological and environmental uses for trivalent metals (like Fe^{3+}, Al^{3+}, and Cr^{3+}) within our daily lives. Being able to detect them and understanding their importance of them becomes crucial in our understanding of the world that surrounds us. Many of these trivalent metals can cause harm when found in deficiency or excess within their surroundings, or even in our own bodies.

Al^{3+} is important due to its massive abundance within the environment and biological relevance. Excess of Al^{3+} within our own bodies can cause significant damage to cells and tissues, and cause a variety of diseases like Parkinson's disease [1]. Another metal of focus is Cr^{3+}, due to its links with many diseases regarding the digestive pathway and cardiovascular system [2]. Lastly Fe^{3+}, excess or deficiency in this metal can cause detrimental damage to one's body. Excess of Fe^{3+} in the body can cause it to become a reactive oxygen species, which can damage proteins, lipids, and nucleic acids found within the body. Deficiency of Fe^{3+} can lead to immunity and blood pressure issues [3].

Significant research has been done regarding trivalent metal colorimetric and fluorometric chemosensors, but many have complex syntheses to obtain their ligand [7-14]. Many have utilized Rhodamine and its derivatives as their ligand to expand on different dyes/ligands that could be used for such chemosensors [7, 9]. Another ligand that has been explored is Schiff-based chemosensors which contain a double bond between nitrogen and carbon and have shown to be successful as a colorimetric and fluorometric chemosensor [14]. Even with these Rhodamine-based and Schiff-based chemosensors, they proven to still have complex ligand synthesis with high limits of detection, ranging from 0.086μM to 20μM [7].

Having a low detection limit for the ligand becomes important in chemosensor research because it allows a consistent reading of the analyte (trivalent metal) at low concentrations. While having a simple synthesis would cut down on the time and resources needed to create these ligands. Being able to detect these trivalent metals, in the environmental and medical aspects, would allow for advancements in research regarding the impacts of these metals in the environment and help with medical diagnoses and imagining. Creating a colorimetric and fluorometric chemosensor that has a simple synthesis, low limits of detection (less than 1μM), and is selective/sensitive to trivalent metals (Al^{3+}, Fe^{3+}, and Cr^{3+}) will prove useful for later applications within the environmental and medical fields.

CHAPTER 2: EXPERIMENTAL

2.1 Materials

The reagents used for synthesis were hydrazine hydrate, 100% (Acros Organics), ethanol (Sigma-Aldrich), and 4-Dimethylanimobenzaldehyde (Sigma-Aldrich). Methanol, HPLC grade, 99.99% (Sigma-Aldrich) was used as diluting solvent for all experiments. Aluminum nitrate nonahydrate 99.997%, and Chromium (III) nitrate nonahydrate 99.99% were both sourced from Sigma-Aldrich. Iron (III) chloride hexahydrate, 99+% for analysis was sourced from Acros Organics.

2.2 Instrumentation

All absorbance measurements were taken on the UV-1800 by Shimadzu, set to collect data within the visible light range (300nm-700nm) and all fluorescence measurements were taken on Fluorolog 322 by Horiba, set to collect data at emission within the 500nm-700nm and the excitation wavelength usually falling around 350nm-400nm. Absorbance measurements were recorded at 497nm and intensity measurement were recorded at 600nm.

2.3 Methods

2.3a. Synthesis of Dye

In Yu et. al, 2012, a simple synthesis for a dye solution was performed [4]. We utilized the same synthesis for our dye to act as the ligand for trivalent metal ion binding. In 50 mL of ethanol, (1.25g, 7 mmol) 4-Dimethylaminobenzaldehyde was dissolved. To this solution, 165 µL (3.4 mmol, 100%) Hydrazine hydrate was added dropwise while being stirred at room temperature. The solution was left overnight to allow for crystallization. The precipitate was vacuum filtered after 24 hours with ethanol and left on the filter for around 20 minutes for the crystals to be fully dry.

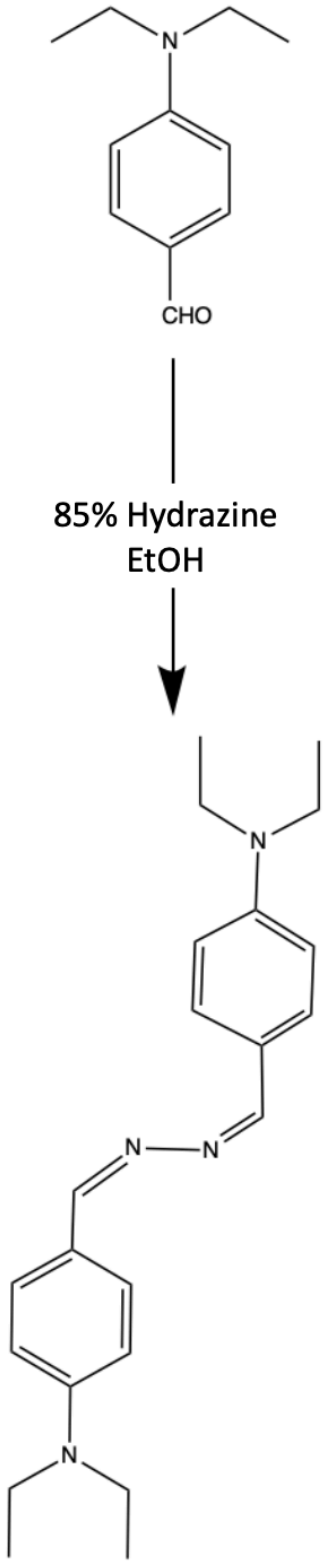

Figure 1: Dye (ligand) synthesis reaction schematic.

2.3b. Job's Plot

Job's Plots were obtained using 10μM M^{3+}, 10μM dye, and diluted with Methanol (MeOH). While lowering the volumes of dye (initial volume of 3000μL, final volume of 0μL), the volume of metal increased (initial volume of 0μL, final volume of 3000 μL). Each solution was prepared such that there was a combination of both the M^{3+} and dye (added up to 3000μL). Solutions were prepared and immediately measured. Job's Plots were obtained in this fashion for both absorbance and fluorescence.

2.3c. Calibration Curve

Calibration curves are performed in triplicate to find the average absorption/intensity to plot against the concentration. Solutions were prepared using 1 mmol dye and 1 mmol M^{3+}, with a range of 1-5 μM of M^{3+} and a constant of 5 μM of dye to plot the calibration curve for each metal.

2.3d. Titrations

Solutions with 10μM dye and 100μM of M^{3+} were used for titrations of all trivalent metals. Starting with 3000μL of 10μM dye, 30 increments of 20μL 100 μM M^{3+} were added and measured at each point to obtain points for titration curves. This same method was used for both absorbance and fluorescence.

2.3e. Precision

The precision experiment was measured as a figure of merit. Solutions of 5μM dye and 0.5μM of M^{3+} were prepared in MeOH(n = 7) and measured for absorbance and intensity. A blank precision experiment was done with just 5 μM of dye diluted with MeOH (n = 7) and measured for absorbance and intensity. Precision was calculated from the average and standard deviation.

CHAPTER 3: RESULTS AND DISCUSSION

All recorded results are found in supplemental data.

3.1 Synthesis of dye/ Percent Yield

The dye synthesis was short with only two steps: mixing reagents at room temperature and crystallizing. While adding the hydrazine hydrate, the purple solution turned to a yellow color, which became even more opaque when left overnight and vacuum-filtered the following day. The yellow crystals were very small and had a powder consistency when dried from the vacuum filtration [4]. After calculating the theoretical yield to be 1.19g, the actual massed-out yield, once filtered and dried, was 0.8987g, resulting in a percent yield of 75.5%.

3.2 Job's Plot

Job's Plots were performed to determine the binding ratio of ligand to M^{3+}. The Job's Plot shows that the binding ratio between the dye and metal was 1:1 [6] for all metals. This relationship is seen in Figure 2, where the peak of the curve is found to be at 0.5 showing that for every 1 mol of ligand added, 1 mol of metal binds to it.

Figure 2: Color change when adding M3+.

When adding M^{3+}, there was a noticeable color change from a light yellow (dye alone) to an orange (when trivalent metal was introduced)

A

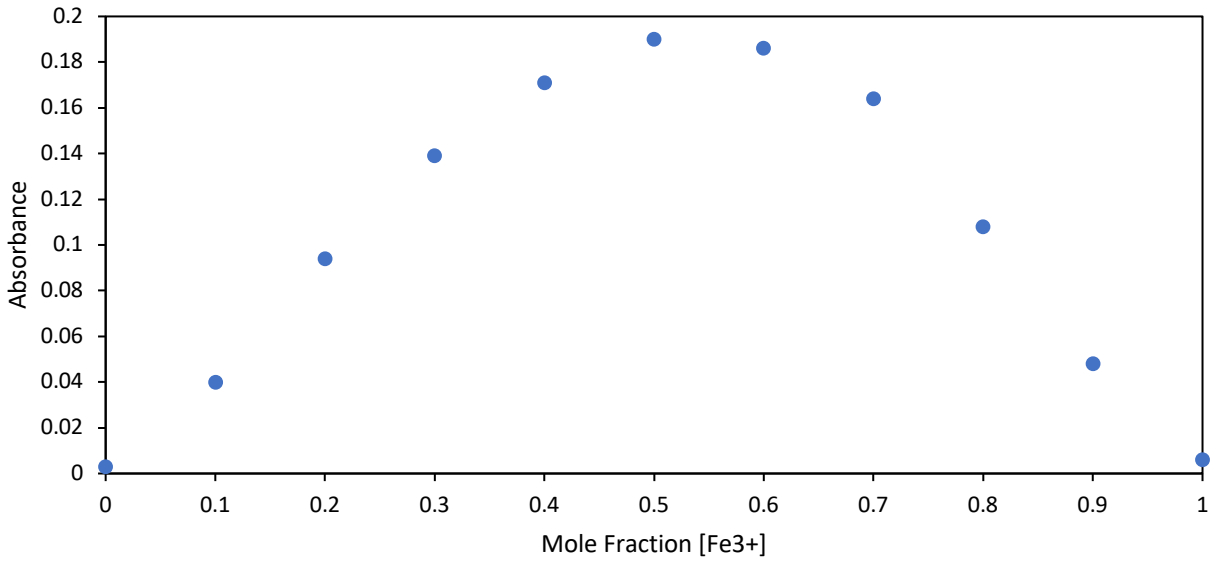

B

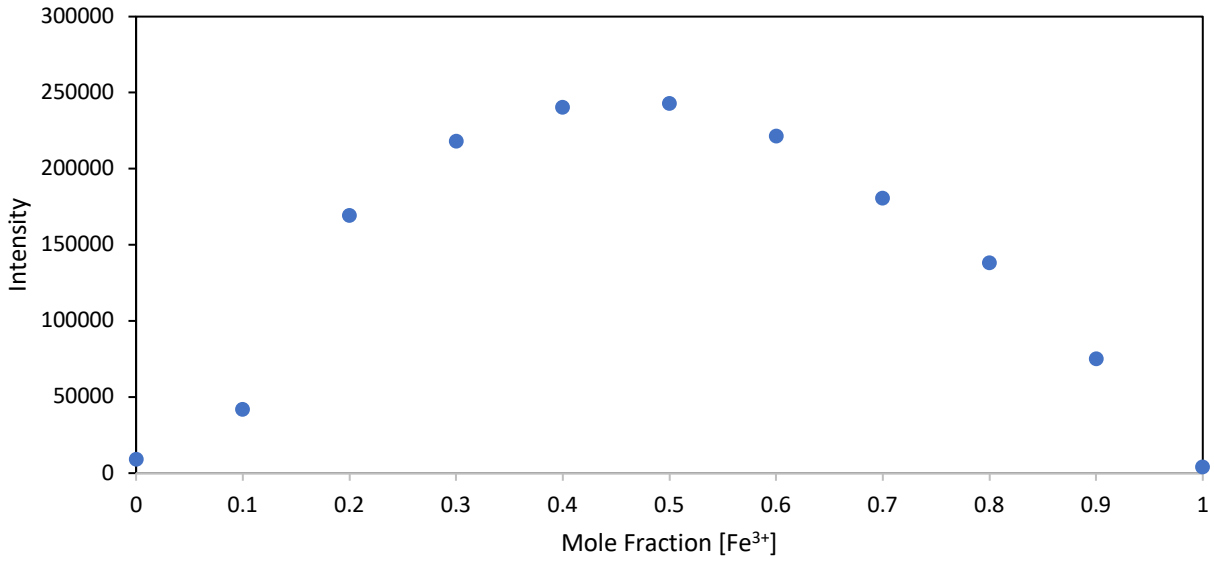

Figure 3: Absorbance and Fluorescence Job's Plots for Fe 3+.

In Plots A and B, 11 solutions of 10 µM Fe^{3+} and 10µM of dye were used in varying increments to find the binding ratio of metal to the ligand.

3.3 Titrations

Finding the equilibrium constant (K_{eq}) of the binding reaction was an important parameter when discussing the chemosensor itself. This was achieved by performing titrations (Figure 3) and finding the K_{eq} with the Benesi-Hildebrand Plot (Figure 4).

While performing the titrations, for absorbance, the peak at 375nm decreased and the peak at 497 nm increased. In addition, a color change was noted from a light yellow to an orange solution the more M^{3+} was added.

Noting that there was an increase in the signal found in the fluorescence titration plot (Figure 3) indicated that this is a turn-on chemosensor and a signal change found within the absorbance titration indicated colorimetric change, that could be seen with the naked eye in the solution. Addition of the metal ion also causes a signal for the analyte to fluoresce. Without the metal, no fluorescence is seen of just the ligand by itself, and when adding the M^{3+} the signal increases (Figure 3) until the ligand is completely saturated and the signal flattens out.

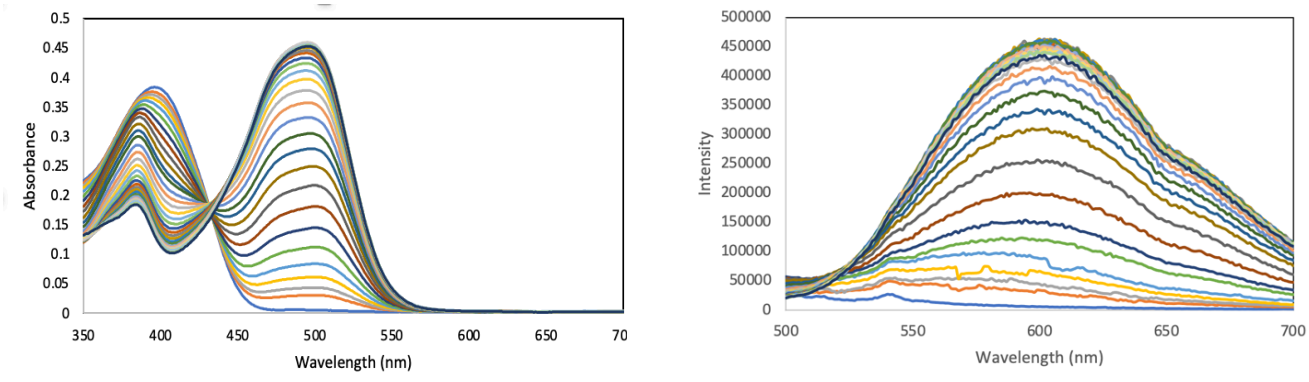

Figure 4: Absorbance and Fluorescence Titration Series Spectra of Fe3+.

Raw data of titrations. The titration curve was achieved with an initial solution containing only 10µM of dye. Thirty increments (20µL) of 100µM Fe^{3+} were added to the dye solution

A

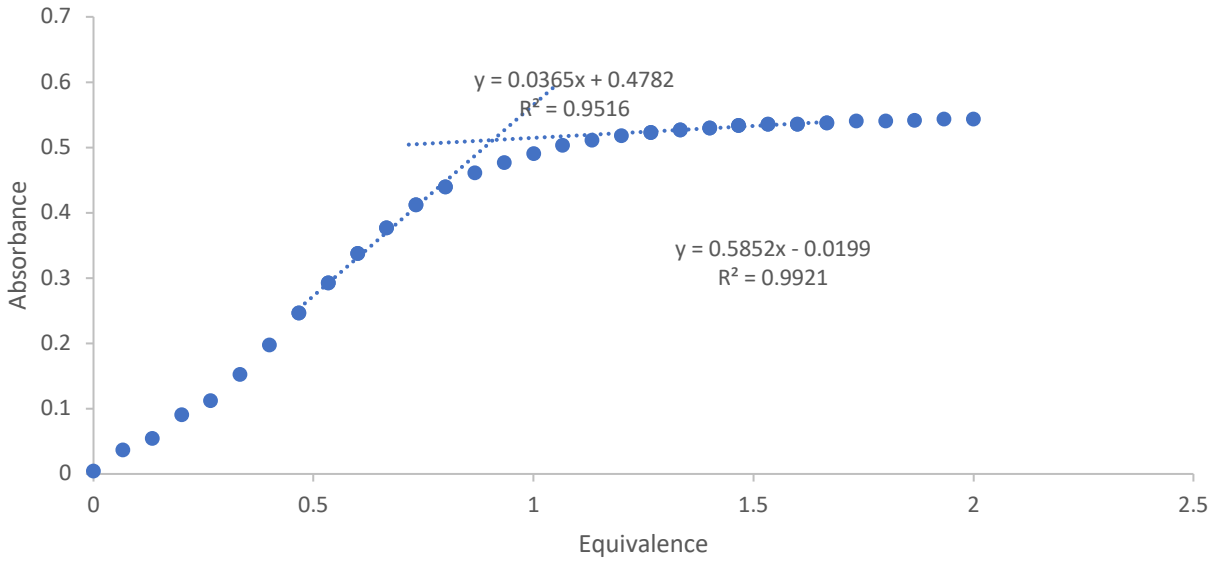

B

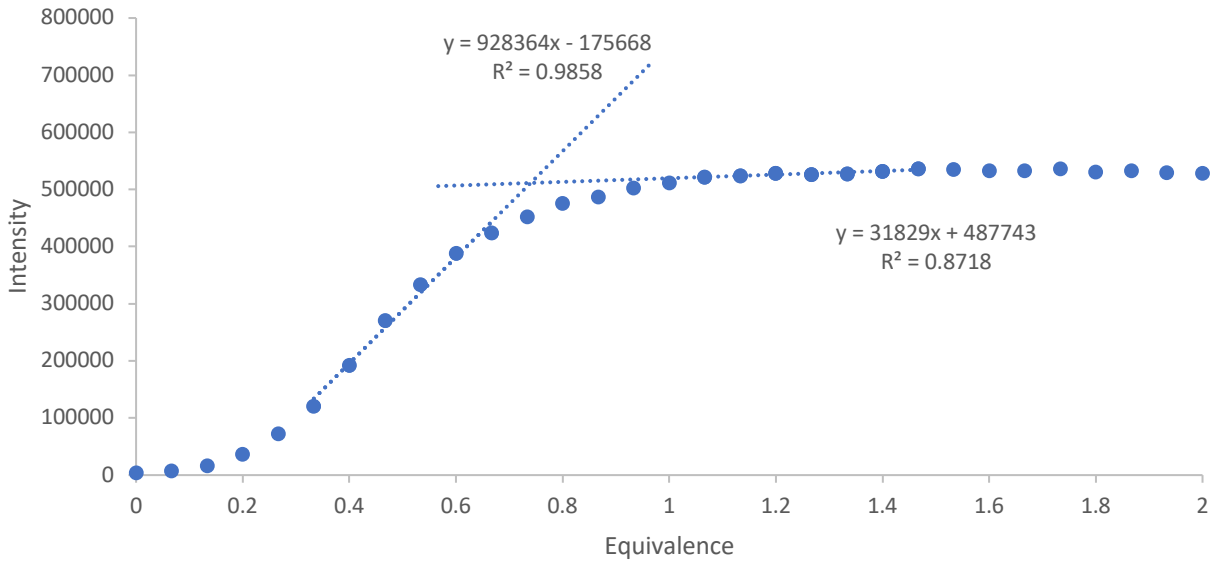

Figure 5: Absorbance and Fluorescence Titration of Fe^{3+}.

The titration curve was achieved with an initial solution containing only 10µM of dye. Thirty increments (20µL) of 100µM Fe^{3+} were added to the dye solution. The equivalence of added metal was calculated to show the binding ratio of metal to the ligand.

From the Titration curves, a Benesi-Hildebrand plot was made to find the equilibrium constant (K_{eq}). The inverse concentration of the M^{3+} concentration was plotted against the inverse of the absorbance subtracted from the initial absorbance/intensity (dye alone). The linear portion of the data was plotted, and the slope and y-intercept were calculated to find the K_{eq}. All K_{eq} values are found in Table 1.

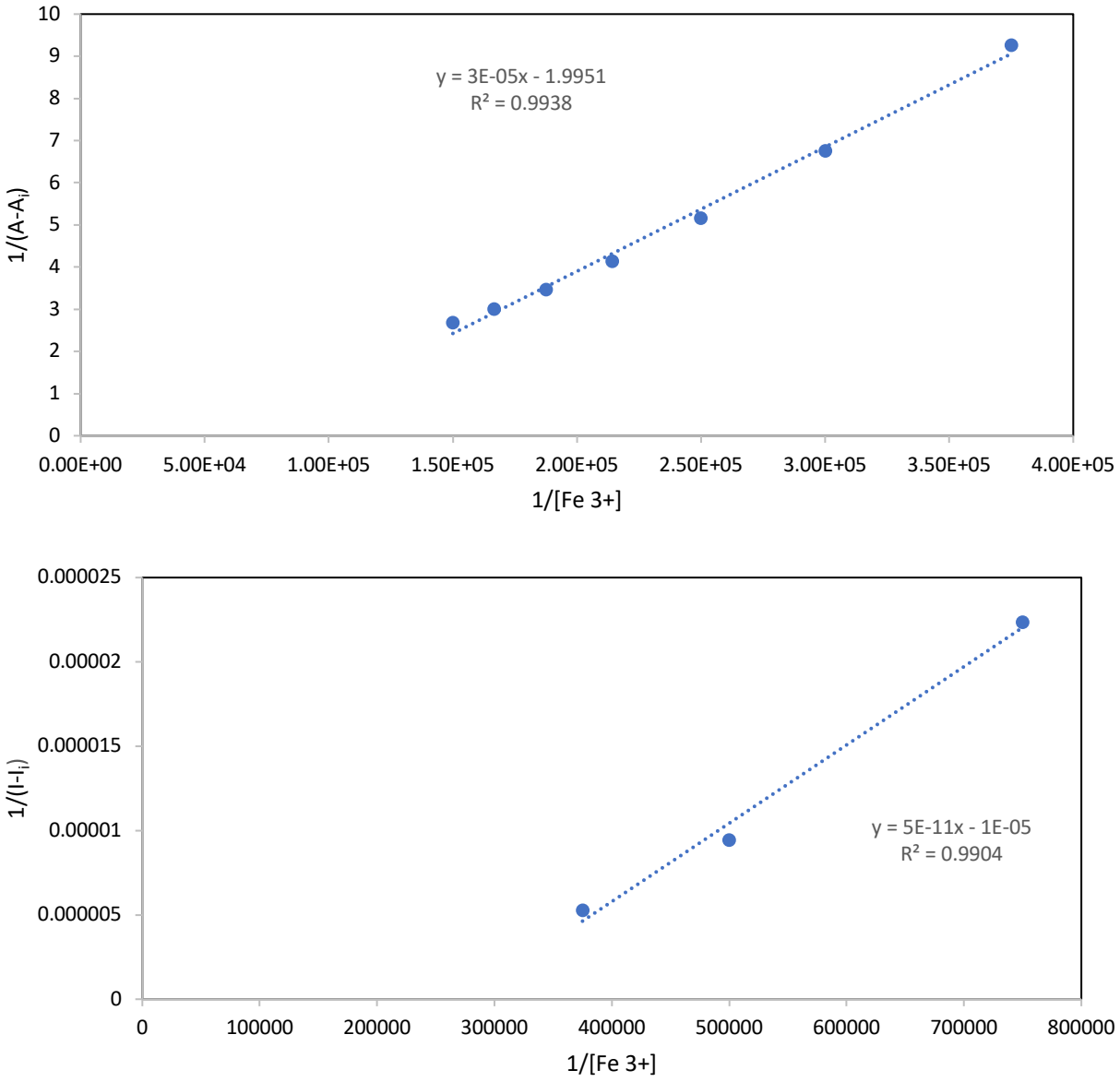

Figure 6: Absorbance and fluorescence Benesi-Hildebrand Plot for Fe^{3+}.

Metal	LOD (μM)		K_{eq} (μM)		% RSD		% recovery	
	ABS	FL	ABS	FL	ABS	FL	ABS	FL
Al^{3+}	0.072	0.016	-3.1E-05	-1.0E-05	15%	9%	103%	96%
Fe^{3+}	0.067	0.019	2.4E-05	-4.9E-06	11%	6%	85%	104%
Cr^{3+}	0.092	0.018	1.2E-05	-1.6E-05	3%	4%	103%	105%

Table 1: Limit of Detection, Keq, precision % RSD, and percent recovery for trivalent metals.

3.4 Accuracy and Precision

Precision experiments were measured as a figure of merit (Table 1). Solutions were prepared and measured immediately. Precision under 10% validates that the data collected is precise. Precision for the dye alone was done to calculate the limit of detection later when the accuracy and calibration curve experiments were performed.

Before measuring more figures of merit to verify the data from above, a calibration curve for each metal was done. Figure 5 shows the calibration curve for Al^{3+}. Utilizing the calibration curve equation, the detection limit was calculated. The limit of detection was calculated with the equation: LOD = 3* SD of blank/slope. The limit of detection for all the trivalent metals was less than 1μM (Table 1), which is a good indicator that with very low concentrations of metal, a consistent detection of the analyte can still be made with the dye that was synthesized. Compared to other literature, the lowest LOD that was found was 0.19μM [14], where the ones obtained for this research all fell below that, ranging from 0.067μM -0.092μM for absorbance and 0.016μM-0.018μM for florescence (Table 1).

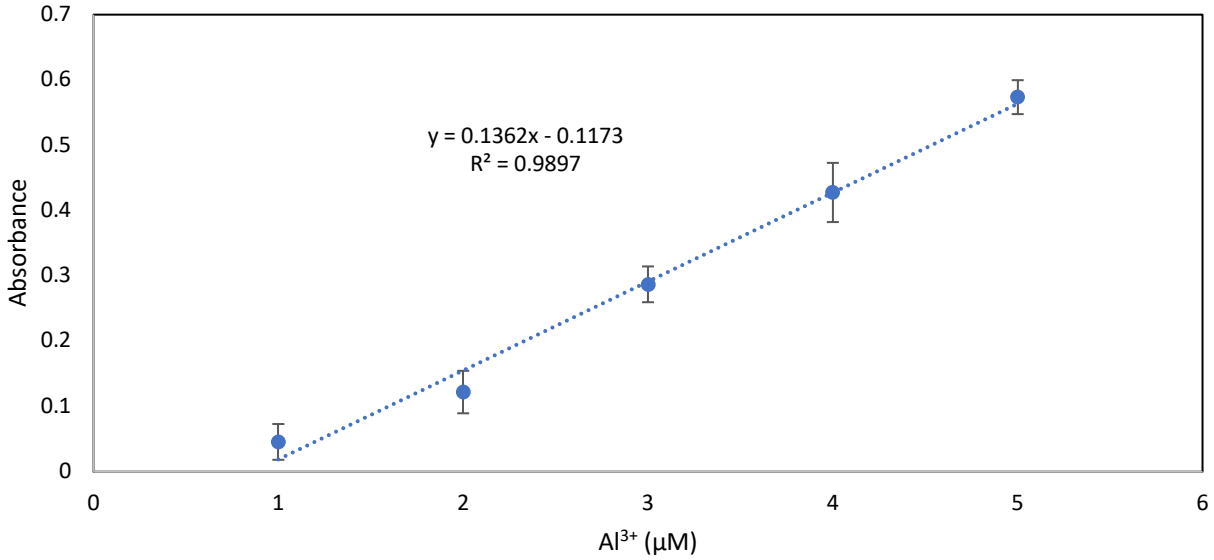

Figure 7: Absorbance Calibration Curve for Al^{3+}.

Solutions of 1mM dye (starting with 250 µL) and 1mM Al^{3+} (10-50 µL) were made, diluted to 10mL with methanol (MeOH), and measured for absorbance to create a calibration curve. The limit of detection (LOD) was then calculated from the curve with the equation: LOD = 3* SD dye/slope, to determine the lowest concentration of metal in the sample which can be detected consistently.

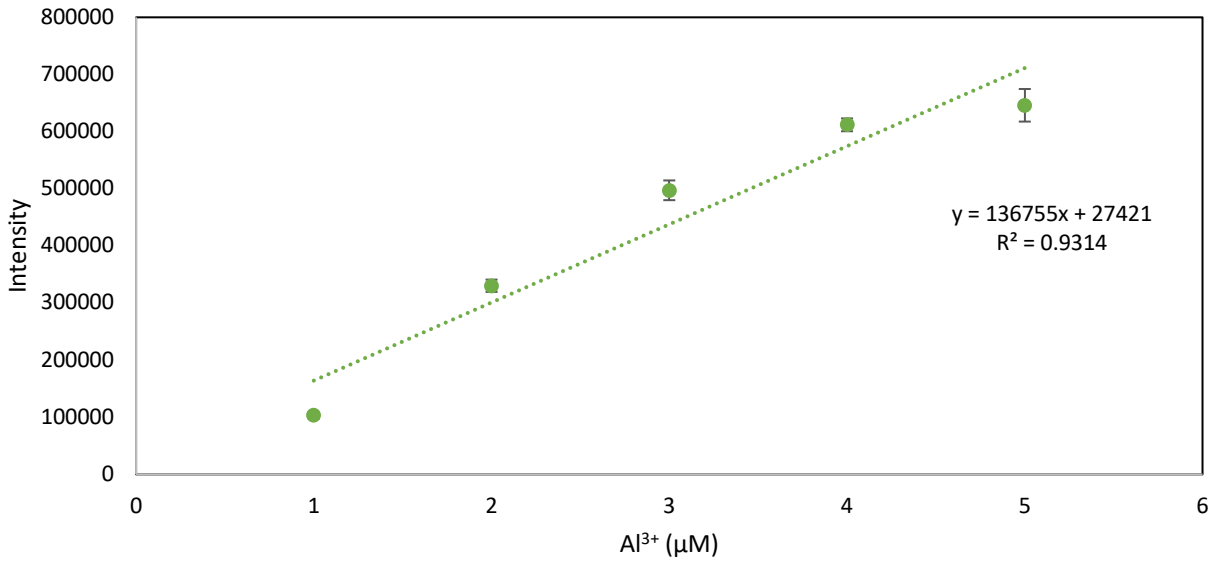

Figure 8: Fluorescence Calibration Curve for Al^{3+}.

Solutions of 1mM dye (starting with 250 µL) and 1mM Al^{3+} (10-50 µL) were made, diluted to 10mL with methanol (MeOH), and measured for intensity to create a calibration curve. The limit of detection (LOD) was then calculated from the curve with the equation: LOD = 3* SD dye/slope, to determine the lowest concentration of metal in the sample which can be detected consistently.

Lastly, accuracy experiments for all the trivalent metals were performed. After noting that the midpoint from the Calibration Curve was found at around 1mM of M^{3+}, the accuracy experiment was utilized as a figure of merit for the project. After collecting all the absorbances and intensity for the three trials, the percent recovery was calculated for each trial and then averaged at the end. A percent recovery of around 90-110% was deemed to be acceptable (Table 1).

CHAPTER 4: CONCLUSION

All of the experiments performed were successful and provided insight into the turn-on fluorescent chemosensor. Through the utilization of Job's Plots and titrations, we were able to determine the binding ratio of all the metals to be 1:1 and that the ligand was a turn-on chemosensor. The K_{eq} for each of the metals was found with the Benesi-Hildebrand Plot. Calibration curves were also made to determine the limit of detection for each metal that showed low numbers. This indicates that the chemosensor would be able to detect trivalent metals at very low concentrations. Lastly, figures of merit experiments were measured to support the data and show precision and accuracy in the data collected.

Overall, the data gives insight into the world of fluorescent chemosensors when detecting trivalent metal ions. With this, more work can be done to show where the metal is binding to within the ligand through the use of NMR. There are proposed areas of binding but very little data to support such ideas. Now being able to detect these trivalent metal ions using fluorescent chemosensors will be useful in the medical field for diagnoses and imaging, and even in environmental applications like water testing. Chemosensor research has made many strides within the last couple of decades, providing a chemosensor with a simple synthesis and low limits of detection provides a step in the right direction and many more things to be discovered.

CHAPTER 5: REFERENCES

1) Inan-Eroglu E, Ayaz A. Is aluminum exposure a risk factor for neurological disorders? J Res Med Sci. 2018 Jun 6;23:51. doi: 10.4103/jrms.JRMS_921_17. PMID: 30057635; PMCID: PMC6040147.
2) Xiangquan Hu, Jie Chai, Yanfei Liu, Bin Liu, Binsheng Yang, Probing chromium(III) from chromium(VI) in cells by a fluorescent sensor, Spectrochimica Acta Part A: Molecular and Biomolecular Spectroscopy, Volume 153, 2016, Pages 505-509, ISSN 1386-1425, https://doi.org/10.1016/j.saa.2015.09.008.
3) Gupta, V. K., Mergu, N., & Kumawat, L. K. (2015, September 15). *A new multifunctional rhodamine-derived probe for colorimetric sensing of Cu(II) and Al(III) and fluorometric sensing of Fe(III) in aqueous media*. Science Direct. file:/// /A_new_multifunctional_rhodamine_derived.pdf
4) Yu, Z., Duan, Y., Cheng, L., Han, Z., Zheng, Z., Zhou, H., Wu, J., & Tian, Y. (2012). Aggregation induced emission in the rotatable molecules: the essential role of molecular interaction. *Journal of Materials Chemistry, 22*, 16927-16932.
5) Hirose, Keiji. (2001). A Practical Guide for the Determination of Binding Constants. Journal of Inclusion Phenomena. 39. 193-209. 10.1023/A:1011117412693.
6) Rodríguez-Cáceres MI, Agbaria RA, Warner IM. Fluorescence of metal-ligand complexes of mono- and di-substituted naphthalene derivatives. J Fluoresc. 2005 Mar;15(2):185-90. doi: 10.1007/s10895-005-2527-1. PMID: 15883774.
7) Wang KP, Chen JP, Zhang SJ, Lei Y, Zhong H, Chen S, Zhou XH, Hu ZQ. Thiophene-based rhodamine as selectivef luorescence probe for Fe(III) and Al(III) in living cells. Anal Bioanal

Chem. 2017 Sep;409(23):5547-5554. doi: 10.1007/s00216-017-0490-8. Epub 2017 Jul 17. PMID: 28717898.

8) Hyun Kim, Kyung Beom Kim, Eun Joo Song, In Hong Hwang, Jin Young Noh, Pan-Gi Kim, Kwang-Duk Jeong, Cheal Kim,Turn-on selective fluorescent probe for trivalent cations, Inorganic Chemistry Communications, Volume 36, 2013, Pages 72-76, ISSN 1387-7003, https://doi.org/10.1016/j.inoche.2013.08.025. (https://www.sciencedirect.com/science/article/pii/S1387700313003365)

9) Shuhua Hou, Zhongguo Qu, Keli Zhong, Yanjiang Bian, Lijun Tang, A new Rhodamine-based visual and fluorometric probe for selective detection of trivalent cations, Tetrahedron Letters, Volume 57, Issue 24, 2016, Pages 2616-2619, ISSN 0040-4039, https://doi.org/10.1016/j.tetlet.2016.04.106.(https://www.sciencedirect.com/science/article/pii/S0040403916304890)

10) Chereddy NR, Nagaraju P, Niladri Raju MV, Krishnaswamy VR, Korrapati PS, Bangal PR, Rao VJ. A novel FRET 'off-on' fluorescent probe for the selective detection of Fe^{3+}, Al^{3+} and Cr^{3+} ions: its ultrafast energy transfer kinetics and application in live cell imaging. Biosens Bioelectron. 2015 Jun 15;68:749-756. doi: 10.1016/j.bios.2015.01.074. Epub 2015 Feb 7. PMID: 25682503.

11) Barba-Bon A, Costero AM, Gil S, Parra M, Soto J, Martínez-Máñez R, Sancenón F. A new selective fluorogenic probe for trivalent cations. Chem Commun (Camb). 2012 Mar 21;48(24):3000-2. doi: 10.1039/c2cc17184h. Epub 2012 Feb 8. PMID: 22318503.

12) Ali, Mahammad & Alam, Rabiul & Bhowmick, Rahul & Islam, Abu & Katarkar, Atul & Chaudhuri, Keya. (2017). A rhodamine based fluorescent trivalent sensor (Fe3+,Al3+,Cr3+) with potential applications for a live cell imaging and combinatorial logic circuit and memory device.. New J. Chem.. 41. 10.1039/C7NJ01675A.

13) Juxiang Meng, Henan Xu, Zhongyu Li, Song Xu, Chao Yao, A turn-on spiropyran derivative based reversible photo-driven colorimetric and fluorescent chemosensor for trivalent metal ions, Tetrahedron, Volume 73, Issue 47, 2017, Pages 6637-6643, ISSN 0040-4020, https://doi.org/10.1016/j.tet.2017.10.014. (https://www.sciencedirect.com/science/article/pii/S0040402017310293)

14) Chandra R, Manna AK, Rout K, Mondal J, Patra GK. A dipodal molecular probe for naked eye detection of trivalent cations (Al^{3+}, $Fe^{3+}$and Cr^{3+}) in aqueous medium and its applications in real sample analysis and molecular logic gates. RSC Adv. 2018 Oct 23;8(63):35946-35958. doi: 10.1039/c8ra07041e. PMID: 35558486; PMCID: PMC9088448.

SUPPLEMENTAL DATA

Figure 3a. Absorbance Job's Plot for Al^{3+}
In the UV-viz, 11 solutions of 10 µM Al^{3+} and 10µM of dye were used in varying increments to find the binding ratio of metal to the ligand.

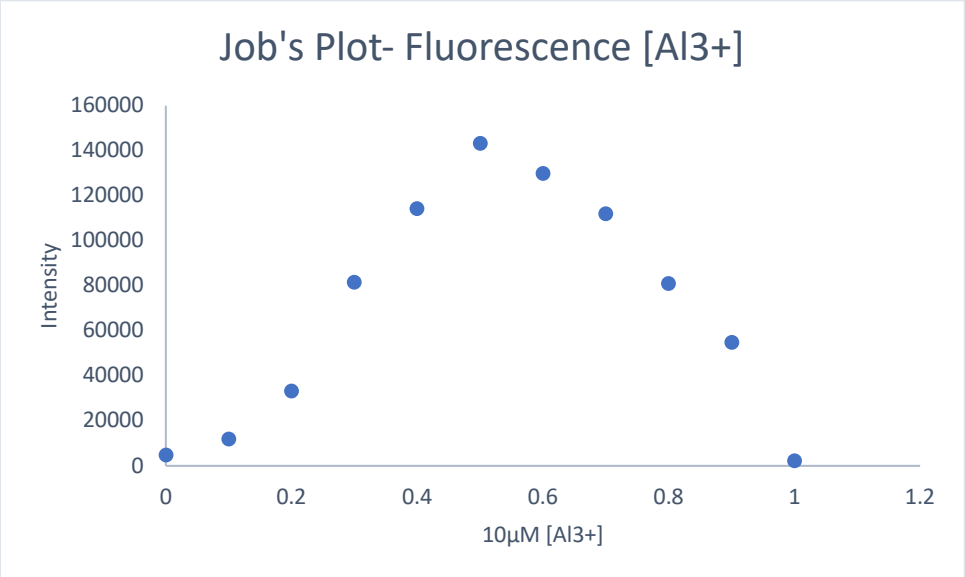

Figure 3b. Fluorescence Job's Plot for Al^{3+}
In the Fluorometer, 11 solutions of 10 µM Al^{3+} and 10µM of dye were used in varying increments to find the binding ratio of metal to ligand.

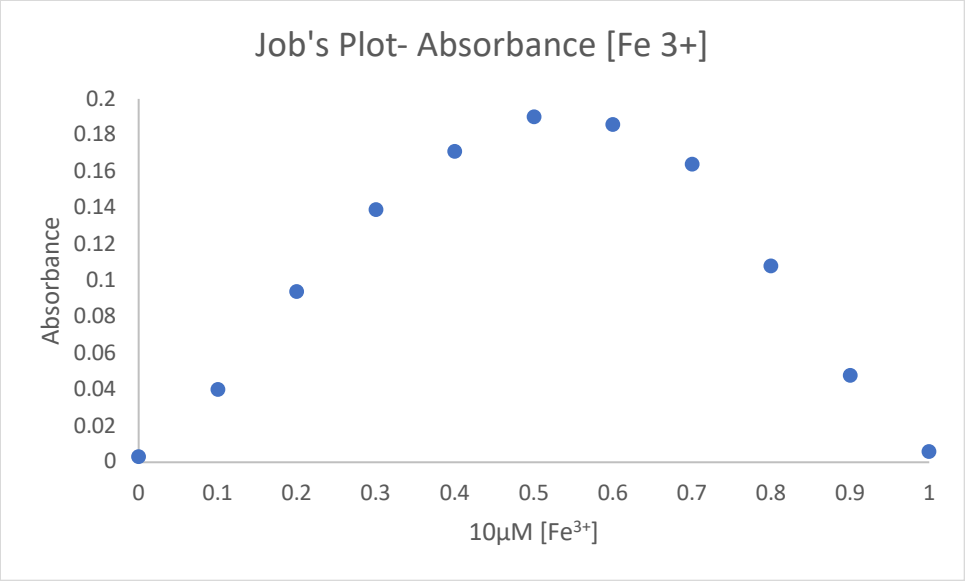

Figure 3c. Absorbance Job's Plot for Fe $^{3+}$
In the UV-viz, 11 solutions of 10 µM Fe $^{3+}$ and 10µM of dye were used in varying increments to find the binding ratio of metal to ligand.

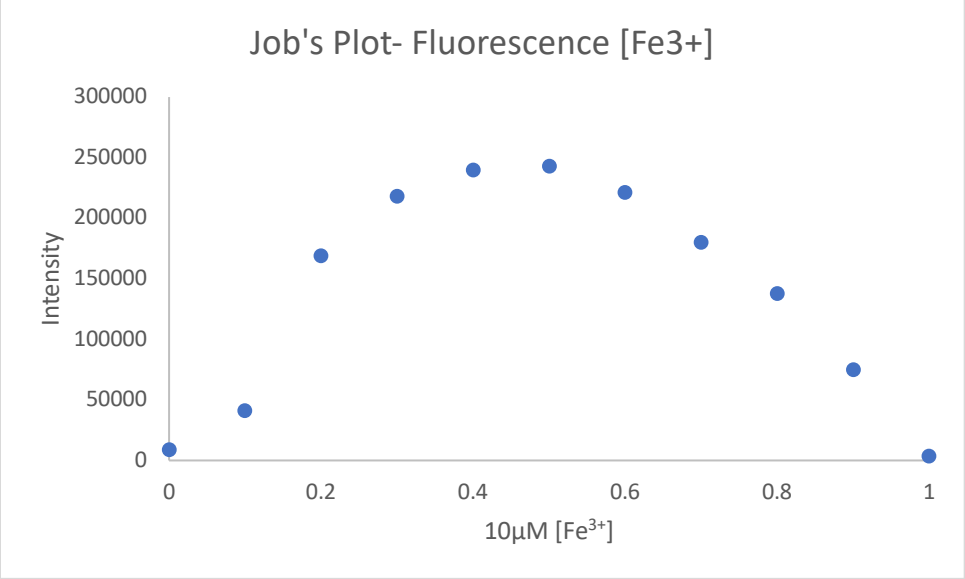

Figure 3d. Fluorescence Job's Plot for Fe $^{3+}$
In the Fluorometer, 11 solutions of 10 µM Fe $^{3+}$ and 10µM of dye were used in varying increments to find the binding ratio of metal to ligand.

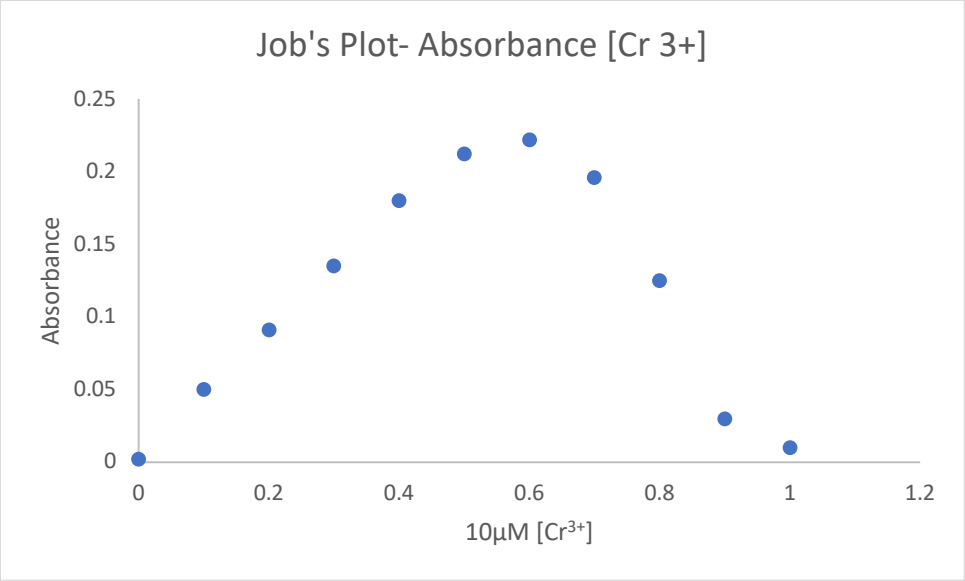

Figure 3e. Absorbance Job's Plot for Cr^{3+}
In the UV-viz, 11 solutions of 10 µM Cr^{3+} and 10µM of dye were used in varying increments to find the binding ratio of metal to ligand.

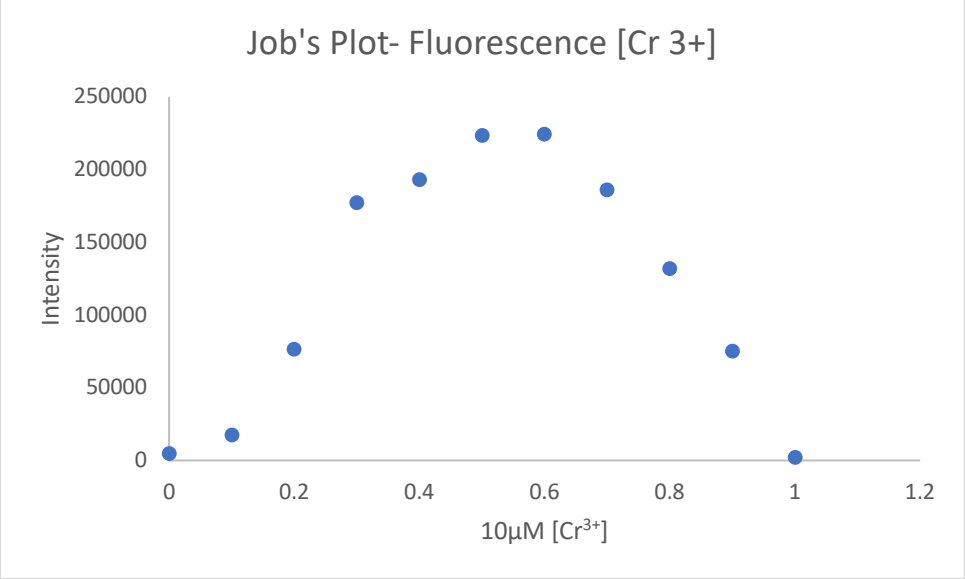

Figure 3f. Fluorescence Job's Plot for Cr^{3+}
In the Fluorometer, 11 solutions of 10 µM Cr^{3+} and 10µM of dye were used in varying increments to find the binding ratio of metal to ligand.

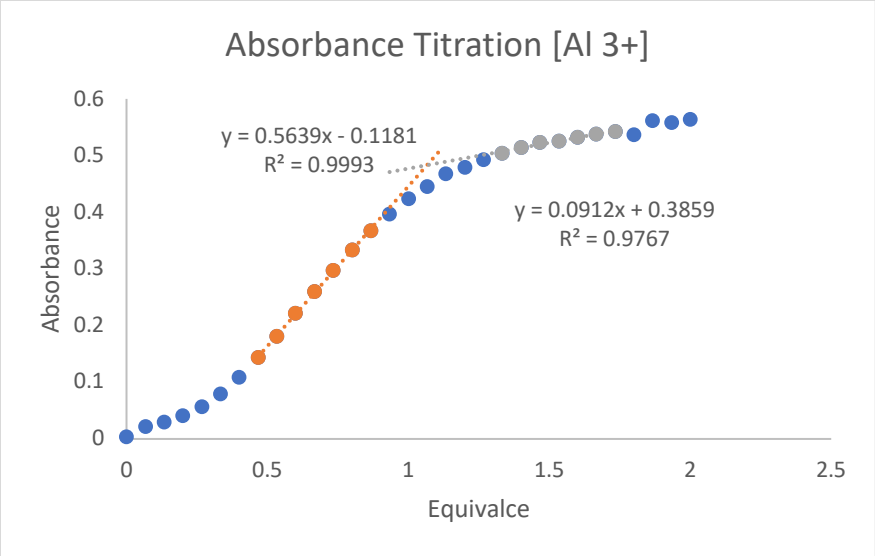

Figure 5a. Absorbance Titration of Al^{3+}

Titration curve was achieved with an initial solution containing only 10µM of dye. Thirty increments of 100µM Al^{3+} (20µL) was added to dye solution. Equivalence of added metal was calculated to show the binding ratio of metal to ligand.

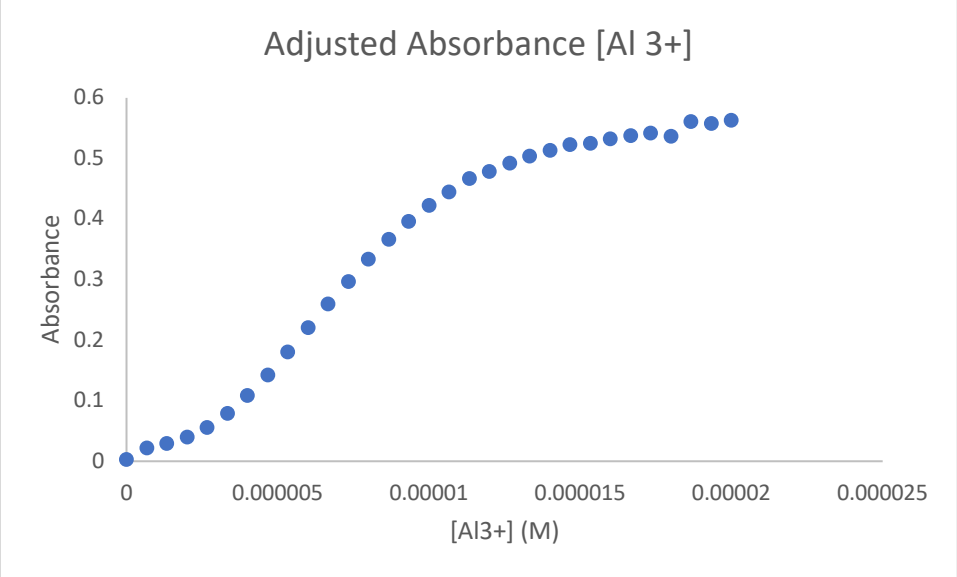

Figure 5b. Adjusted Absorbance of Al^{3+}

To account for the dilution, calculations were performed to graph the adjusted absorbance for each titration point. The formula used for this was:

Absorbance *(µL of metal added + initial volume of dye [V_{int}])/ initial volume of dye [V_{int}]

Which accounted for the dilution concentration of the metal to ligand.

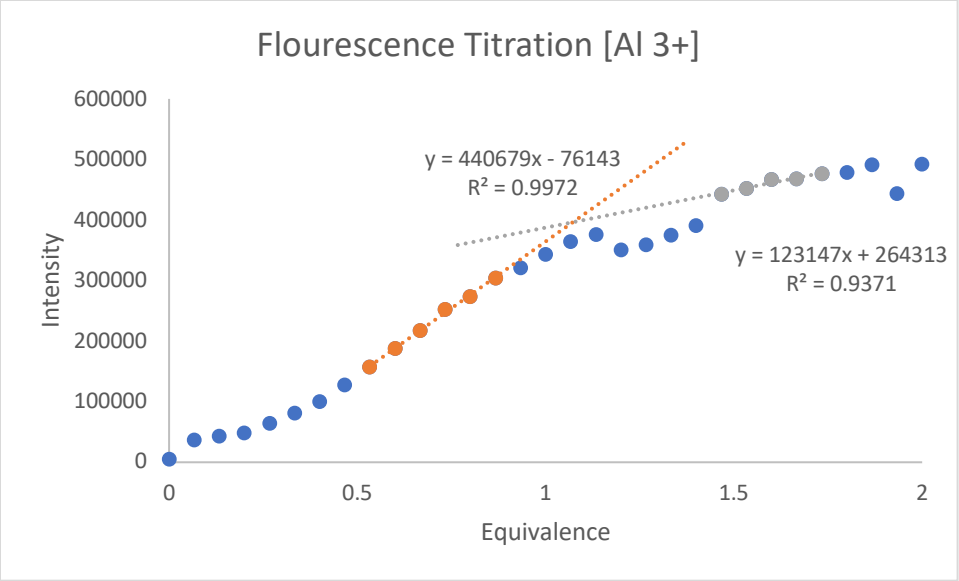

Figure 5c. Fluorescence Titration of Al^{3+}
Titration curve was achieved with an initial solution containing only 10µM of dye. Thirty increments (20µL) of 100µM Al^{3+} was added to dye solution. Equivalence of added metal was calculated to show the binding ratio of metal to ligand.

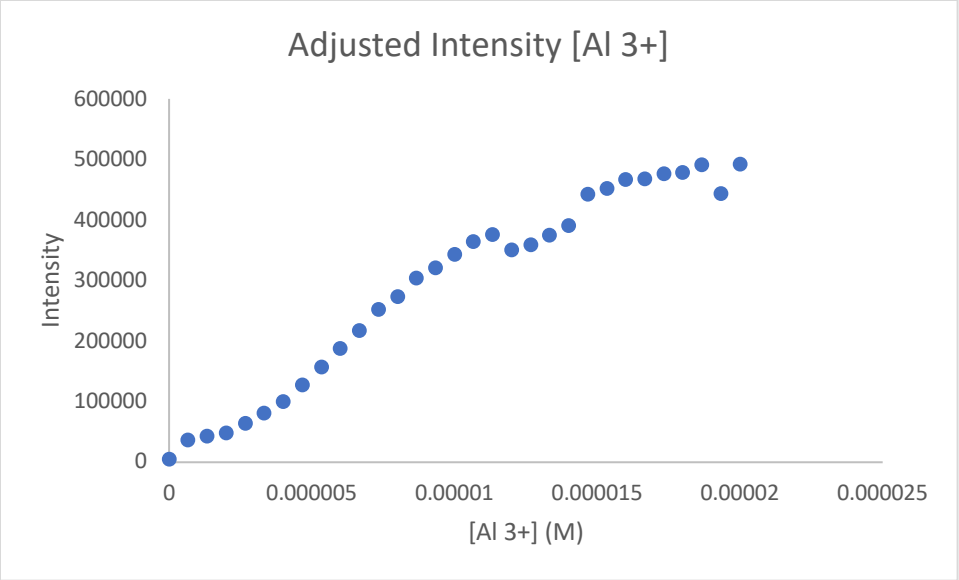

Figure 5d. Adjusted Intensity of Al^{3+}
To account for the dilution, calculations were performed to graph the adjusted absorbance for each titration point. The formula used for this was:
Intensity *(µL of metal added + initial volume of dye [V_{int}])/ initial volume of dye [V_{int}]
Which accounted for the dilution concentration of the metal to ligand.

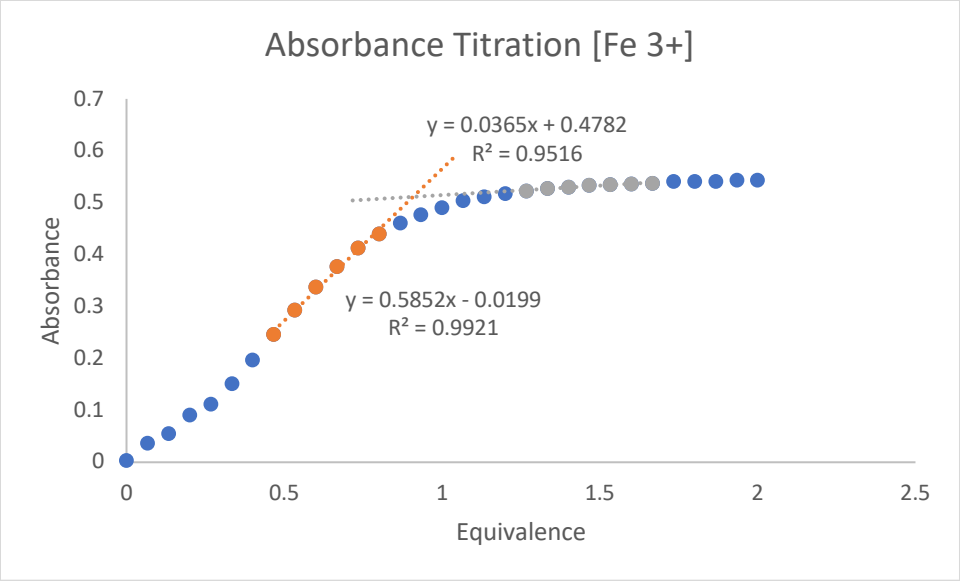

Figure 5e. Absorbance Titration of Fe^{3+}
Titration curve was achieved with an initial solution containing only 10µM of dye. Thirty increments of 100µM Fe^{3+} (20µL) was added to dye solution. Equivalence of added metal was calculated to show the binding ratio of metal to ligand.

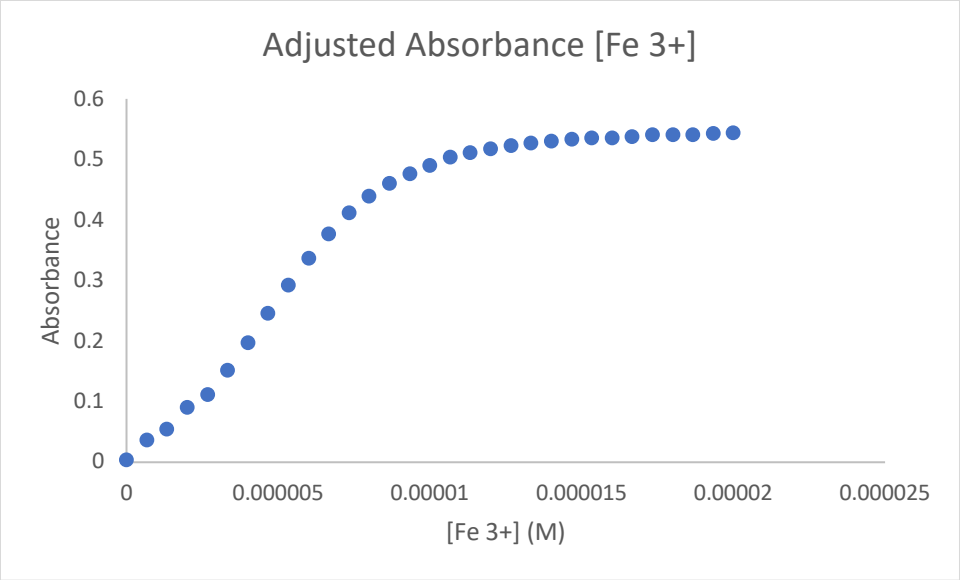

Figure 5f. Adjusted Absorbance of Fe^{3+}
To account for the dilution, calculations were performed to graph the adjusted absorbance for each titration point. The formula used for this was:
Absorbance *(µL of metal added + initial volume of dye [V_{int}])/ initial volume of dye [V_{int}]
Which accounted for the dilution concentration of the metal to ligand.

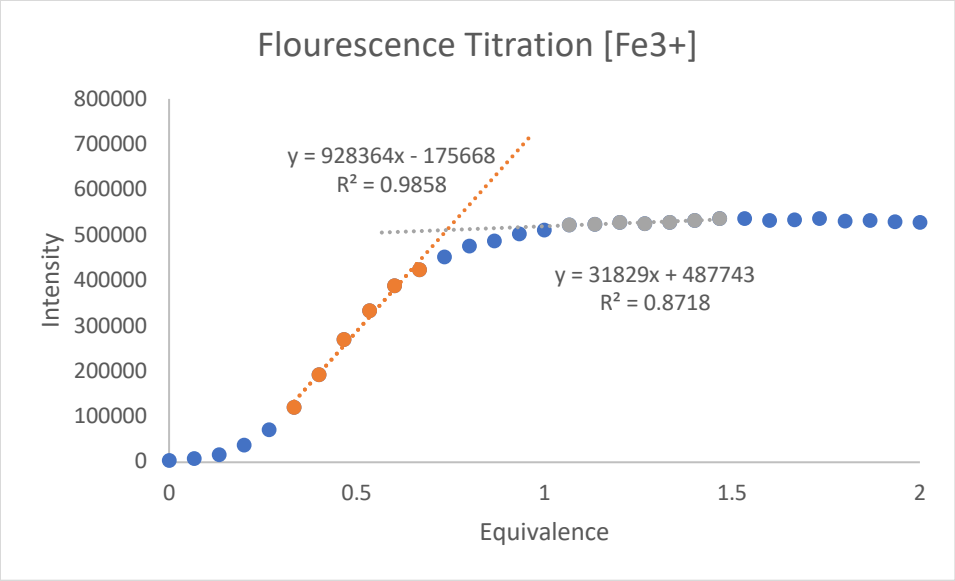

Figure 5g. Fluorescence Titration of Fe^{3+}
Titration curve was achieved with an initial solution containing only 10µM of dye. Thirty increments (20µL) of 100µM Fe^{3+} was added to dye solution. Equivalence of added metal was calculated to show the binding ratio of metal to ligand.

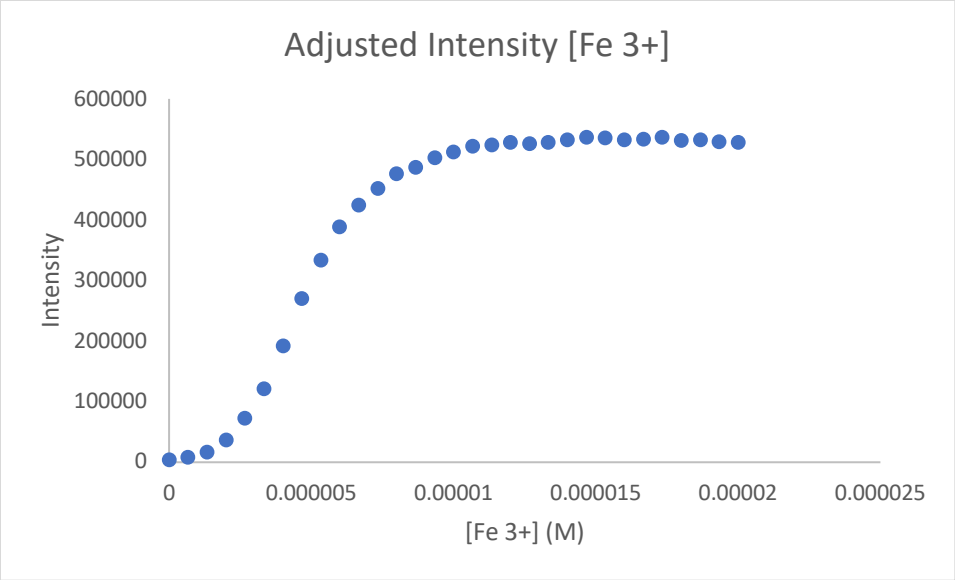

Figure 5h. Adjusted Intensity of Fe^{3+}
To account for the dilution, calculations were performed to graph the adjusted absorbance for each titration point. The formula used for this was:
Intensity *(µL of metal added + initial volume of dye [V_{int}])/ initial volume of dye [V_{int}]
Which accounted for the dilution concentration of the metal to ligand.

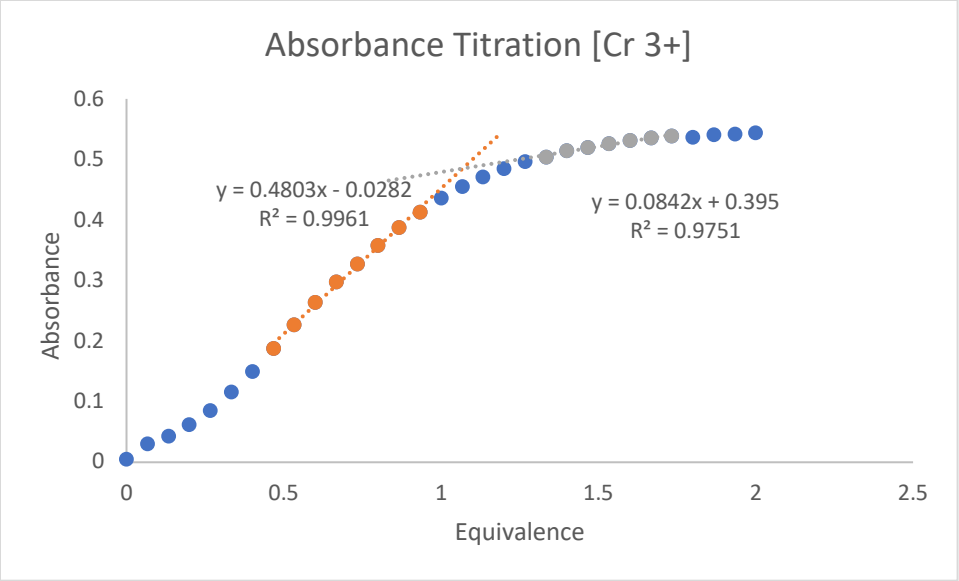

Figure 5i. Absorbance Titration of Cr^{3+}
Titration curve was achieved with an initial solution containing only 10µM of dye. Thirty increments of 100µM Cr^{3+} (20µL) was added to dye solution. Equivalence of added metal was calculated to show the binding ratio of metal to ligand.

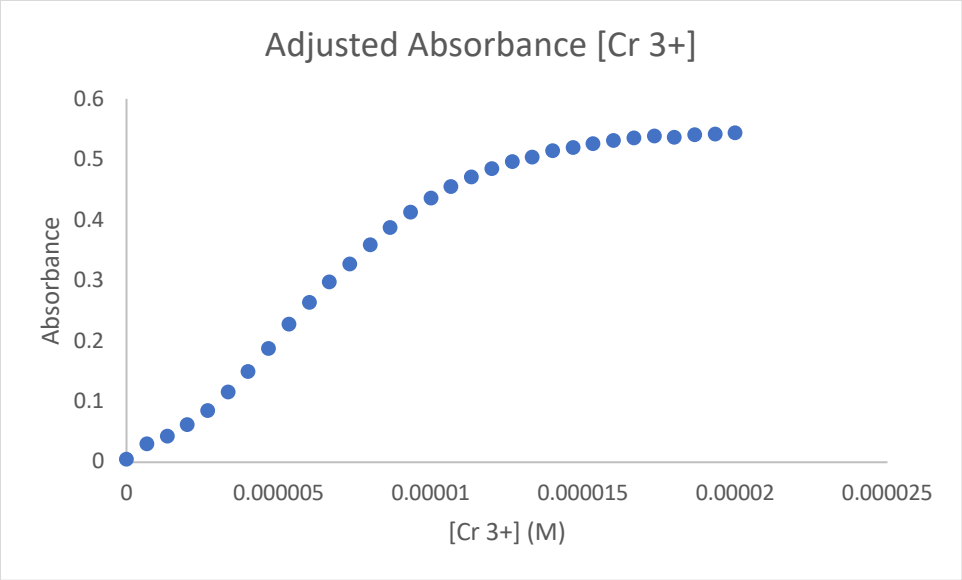

Figure 5j. Adjusted Absorbance of Cr^{3+}
To account for the dilution, calculations were performed to graph the adjusted absorbance for each titration point. The formula used for this was:
Absorbance *(µL of metal added + initial volume of dye [V_{int}])/ initial volume of dye [V_{int}]
Which accounted for the dilution concentration of the metal to ligand.

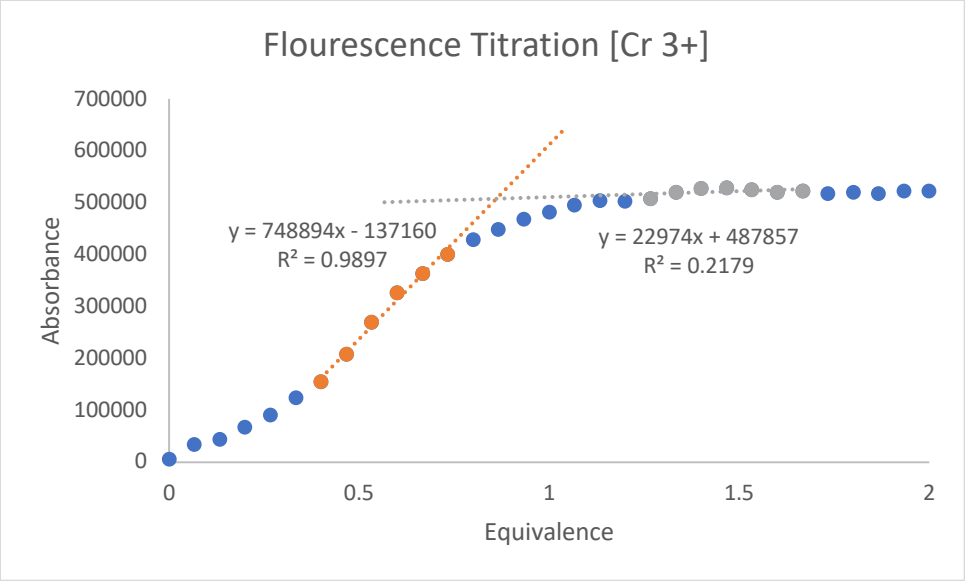

Figure 5k. Fluorescence Titration of Cr^{3+}
Titration curve was achieved with an initial solution containing only 10µM of dye. Thirty increments (20µL) of 100µM Cr^{3+} was added to dye solution. Equivalence of added metal was calculated to show the binding ratio of metal to ligand.

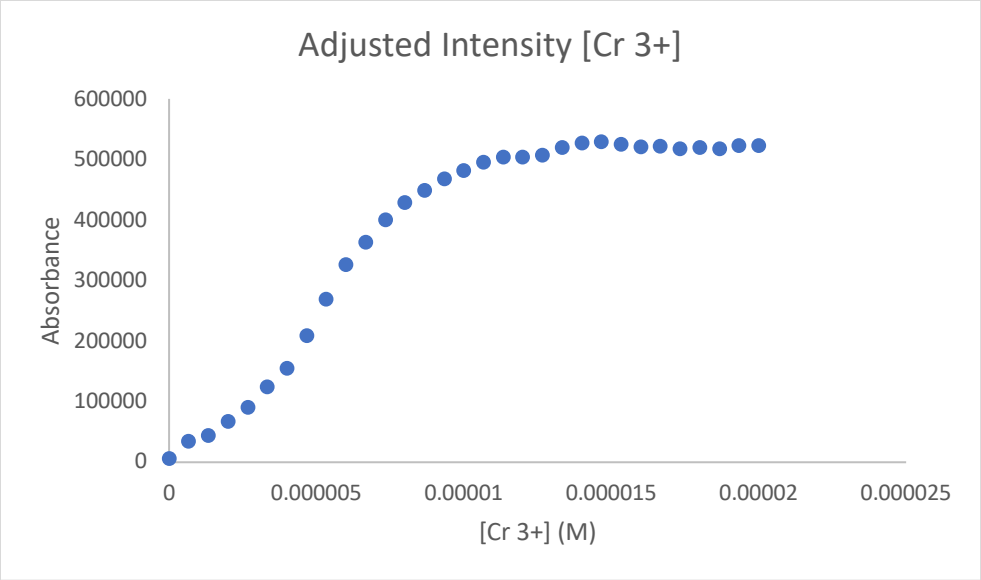

Figure 5l. Adjusted Intensity of Cr^{3+}
To account for the dilution, calculations were performed to graph the adjusted absorbance for each titration point. The formula used for this was:
Intensity *(µL of metal added + initial volume of dye [V_{int}])/ initial volume of dye [V_{int}]
Which accounted for the dilution concentration of the metal to ligand.

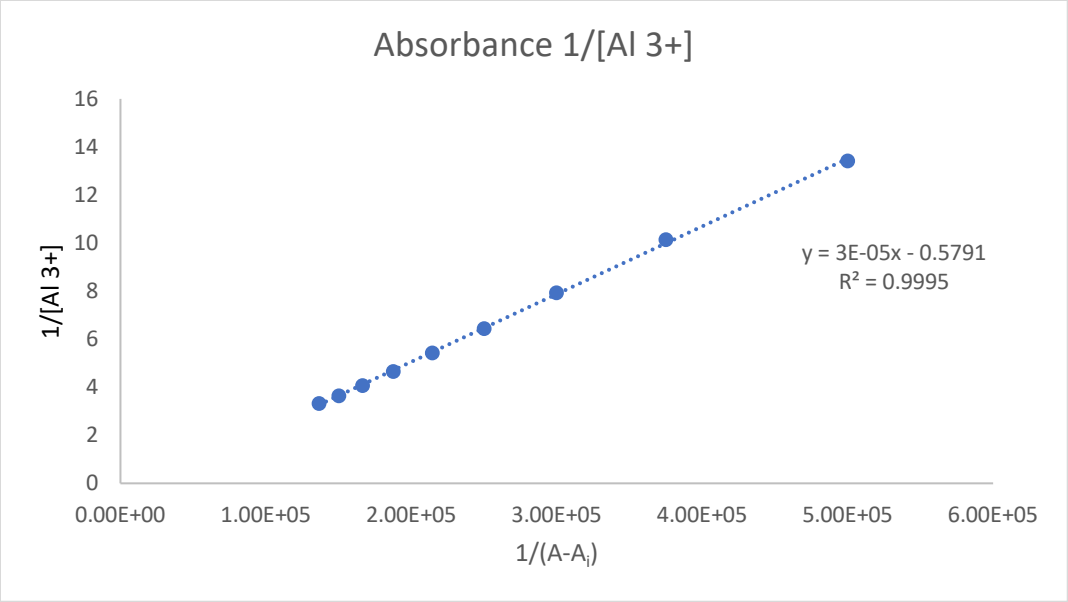

Figure 6a. Absorbance Benesi-Hildebrand Plot for Al^{3+}

Calculations were made from the observed absorbance from the titration data to achieve the Benesi-Hildebrand plot. The inverse of adjusted absorbance was plotted against 1/ (absorbance observed- absorbance of dye alone). The linear portion of the data was then plotted.

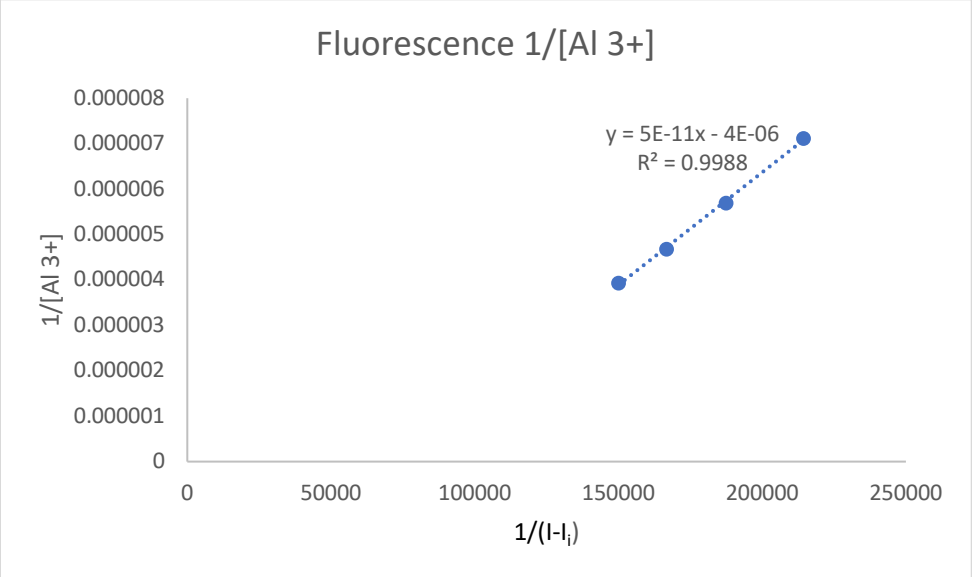

Figure 6b. Fluorescence Benesi-Hildebrand Plot for Al^{3+}

Calculations were made from the observed intensity from the titration data to achieve the Benesi-Hildebrand plot. The inverse of adjusted absorbance was plotted against 1/ (intensity observed- intensity of dye alone). The linear portion of the data was then plotted.

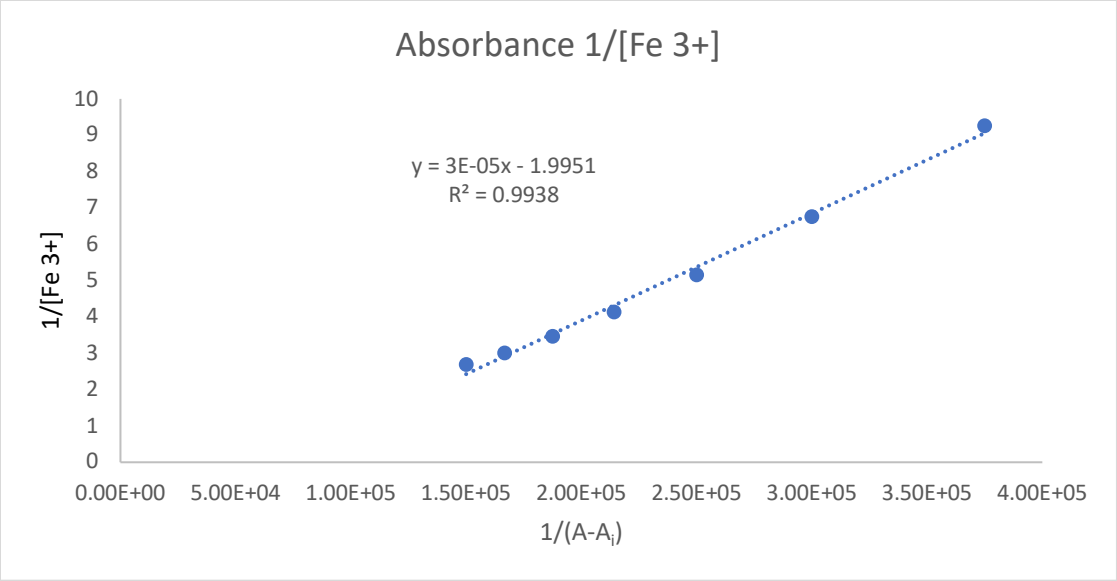

Figure 6c. Absorbance Benesi-Hildebrand Plot for Fe^{3+}

Calculations were made from the observed absorbance from the titration data to achieve the Benesi-Hildebrand plot. The inverse of adjusted absorbance was plotted against 1/ (absorbance observed- absorbance of dye alone). The linear portion of the data was then plotted.

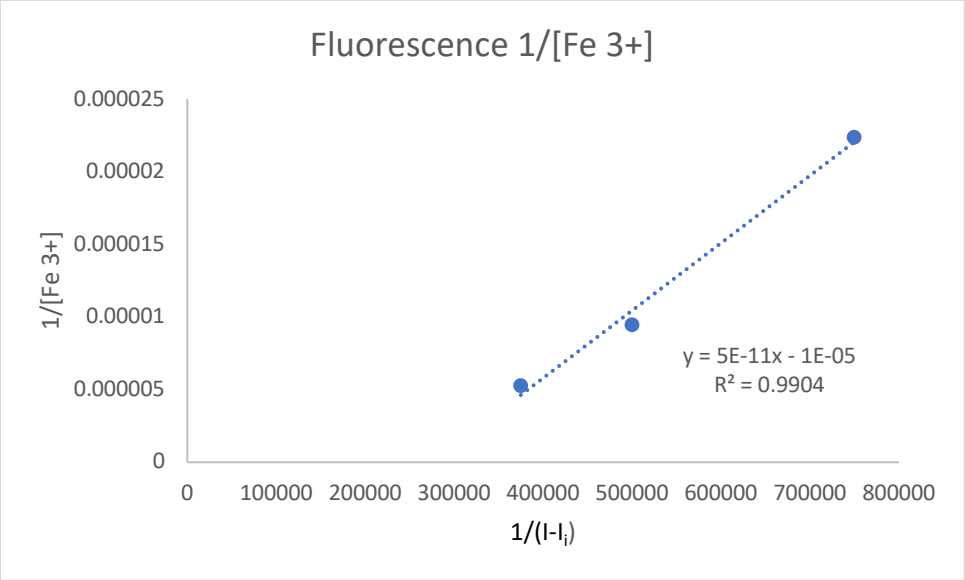

Figure 6d. Fluorescence Benesi-Hildebrand Plot for Fe^{3+}

Calculations were made from the observed intensity from the titration data to achieve the Benesi-Hildebrand plot. The inverse of adjusted absorbance was plotted against 1/ (intensity observed- the intensity of dye alone). The linear portion of the data was then plotted.

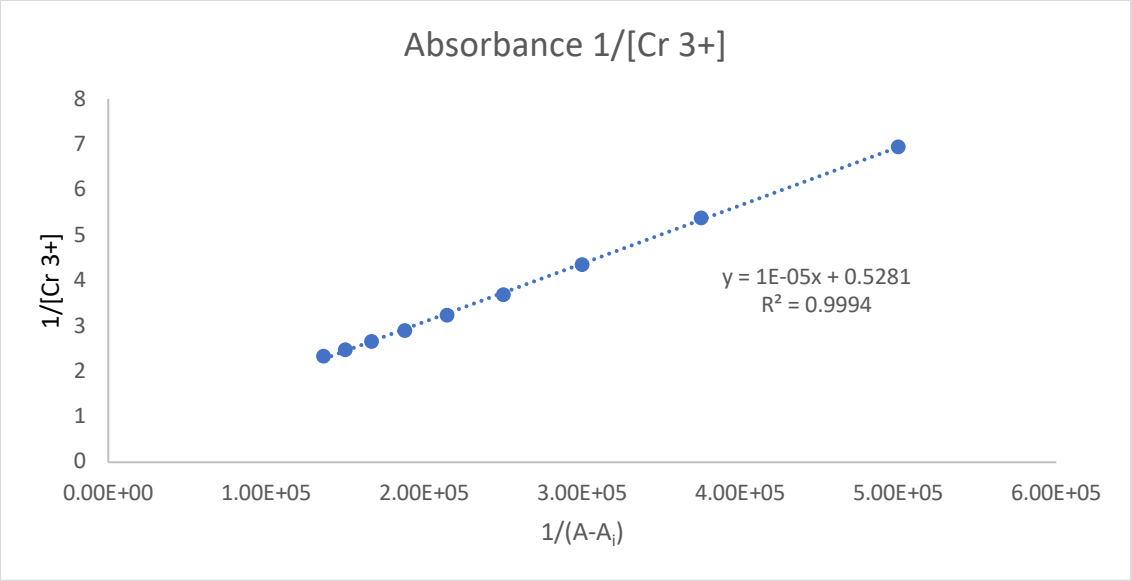

Figure 9a. Absorbance Benesi-Hildebrand Plot for Cr^{3+}

Calcula6eons were made from the observed absorbance from the titration data to achieve the Benesi-Hildebrand plot. The inverse of adjusted absorbance was plotted against 1/ (absorbance observed- absorbance of dye alone). The linear portion of the data was then plotted.

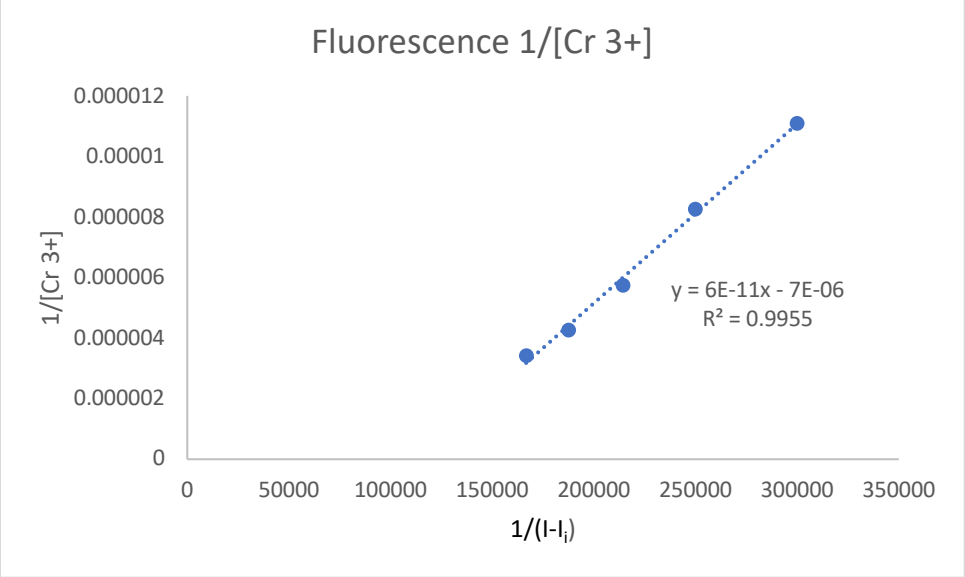

Figure 6f. Fluorescence Benesi-Hildebrand Plot for Cr^{3+}

Calculations were made from the observed intensity from the titration data to achieve the Benesi-Hildebrand plot. The inverse of adjusted absorbance was plotted against 1/ (intensity observed- intensity of dye alone). The linear portion of the data was then plotted.

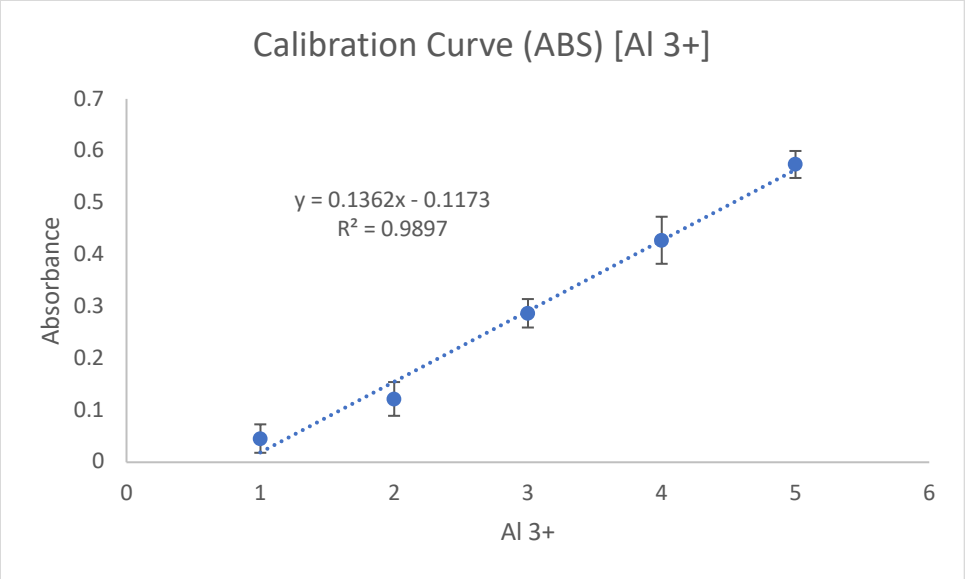

LOD 0.071956

Figure 7a. Absorbance Calibration Curve for Al^{3+}

Solutions of 1mM dye (starting with 250 µL) and 1mM Al^{3+} (10-50 µL) were made, diluted to 10mL with methanol (MeOH), and measured for absorbance to create a calibration curve. The limit of detection (LOD) was then calculated from the curve with the equation:

LOD= 3* SD dye/slope

to determine the lowest concentration of metal in the sample which can be detected consistently.

trial	abs	[Al]	% recovery
1	0.231	2.557895	102%
2	0.227	2.528519	101%
3	0.242	2.638678	106%
	known	2.5	103%

Table 1a. Absorbance Accuracy Experiment for Al^{3+}

Utilizing the calibration curve, the accuracy experiment was performed to ensure that the percent recovery for the sample was accurate (90%-110%). This was achieved by using the same solution as the calibration curve experiment, 1mM dye (250 µL) and 1mM Al^{3+} (25 µL) and diluted with MeOH to the 10mL. Performed in triplicate to get averages and calculate the percent recovery for Al^{3+}.

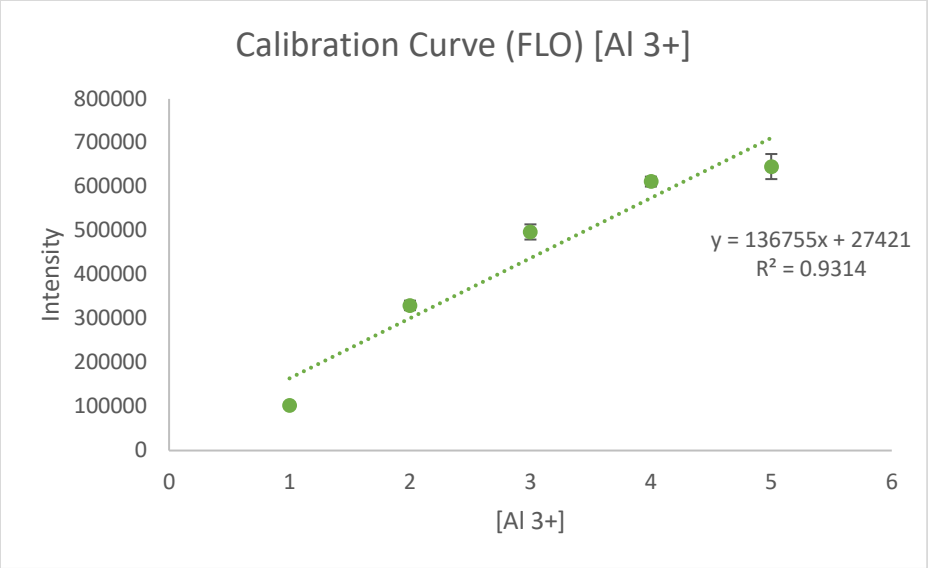

LOD 0.016347454

Figure 7b. Fluorescence Calibration Curve for Al^{3+}

Solutions of 1mM dye (starting with 250 µL) and 1mM Al^{3+} (10-50 µL) were made, diluted to 10mL with methanol (MeOH), and measured for intensity to create a calibration curve. The limit of detection (LOD) was then calculated from the curve with the equation:

LOD= 3* SD dye/slope

to determine the lowest concentration of metal in the sample which can be detected consistently.

trial	abs	[Al 3+]	% recovery
1	360930	2.438725	98%
2	363420	2.456933	98%
3	337510	2.26747	91%
	exp	2.387709	96%
	known	2.5	

Table 1b. Intensity Accuracy Experiment for Al^{3+}

Utilizing the calibration curve, the accuracy experiment was performed to ensure that the percent recovery for the sample was accurate (90%-110%). This was achieved by using the same solution as the calibration curve experiment, 1mM dye (250 µL) and 1mM Al^{3+} (25 µL) and diluted with MeOH to the 10mL. Performed in triplicate to get averages and calculate the percent recovery for Al^{3+}.

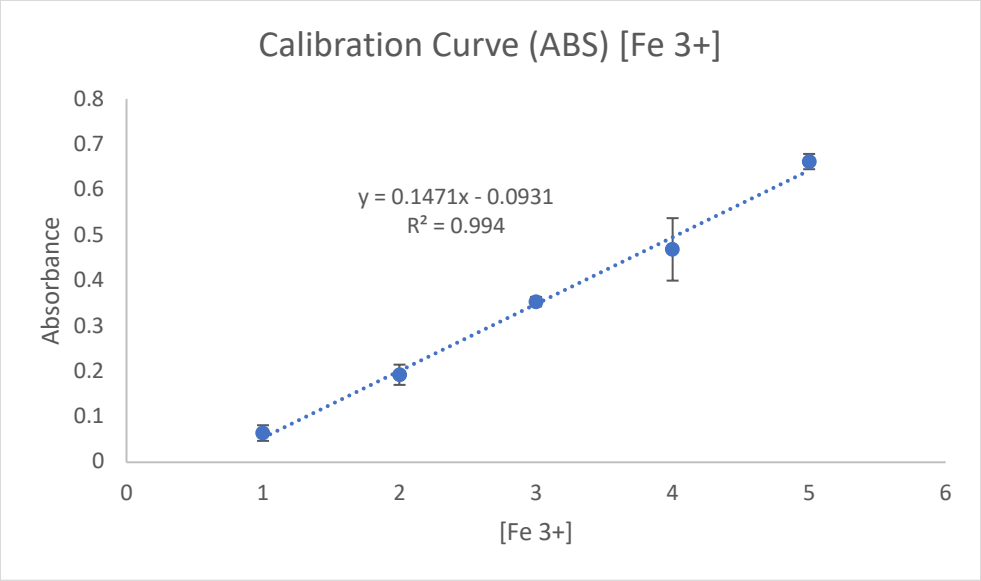

LOD 0.066592

Figure 7c. Absorbance Calibration Curve for Fe^{3+}

Solutions of 1mM dye (starting with 250 µL) and 1mM Fe^{3+} (10-50 µL) were made, diluted to 10mL with methanol (MeOH), and measured for absorbance to create a calibration curve. The limit of detection (LOD) was then calculated from the curve with the equation:

LOD= 3* SD dye/slope

to determine the lowest concentration of metal in the sample which can be detected consistently.

trial	abs	[Fe]	% recovery
1	0.198	1.978704	79%
2	0.207	2.039873	82%
3	0.258	2.386498	95%
	known	2.5	85%

Table 2a. Absorbance Accuracy Experiment for Fe^{3+}

Utilizing the calibration curve, the accuracy experiment was performed to ensure that the percent recovery for the sample was accurate (90%-110%). This was achieved by using the same solution as the calibration curve experiment, 1mM dye (250 µL) and 1mM Fe^{3+} (25 µL) and diluted with MeOH to the 10mL. Performed in triplicate to get averages and calculate the percent recovery for Fe^{3+}.

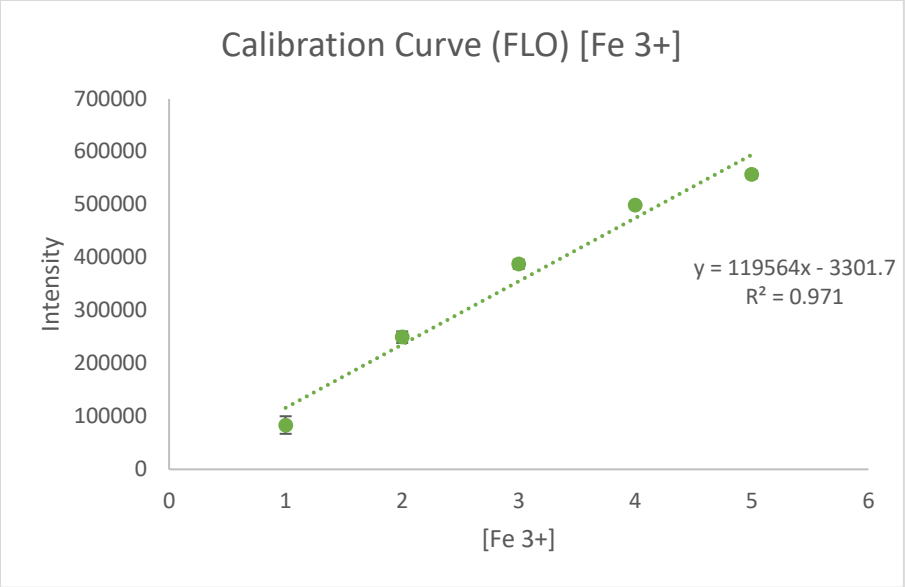

LOD 0.018698

Figure 7d. Fluorescence Calibration Curve for Fe^{3+}

Solutions of 1mM dye (starting with 250 µL) and 1mM Fe^{3+} (10-50 µL) were made, diluted to 10mL with methanol (MeOH), and measured for intensity to create a calibration curve. The limit of detection (LOD) was then calculated from the curve with the equation:

LOD= 3* SD dye/slope

to determine the lowest concentration of metal in the sample which can be detected consistently.

trial	abs	[Fe3+]	% recovery
1	305660	2.584077	103%
2	319330	2.698409	108%
3	301380	2.54828	102%
	exp	2.610255	104%
	known	2.5	

Table 2b. Intensity Accuracy Experiment for Fe^{3+}

Utilizing the calibration curve, the accuracy experiment was performed to ensure that the percent recovery for the sample was accurate (90%-110%). This was achieved by using the same solution as the calibration curve experiment, 1mM dye (250 µL) and 1mM Fe^{3+} (25 µL) and diluted with MeOH to the 10mL. Performed in triplicate to get averages and calculate the percent recovery for Fe^{3+}.

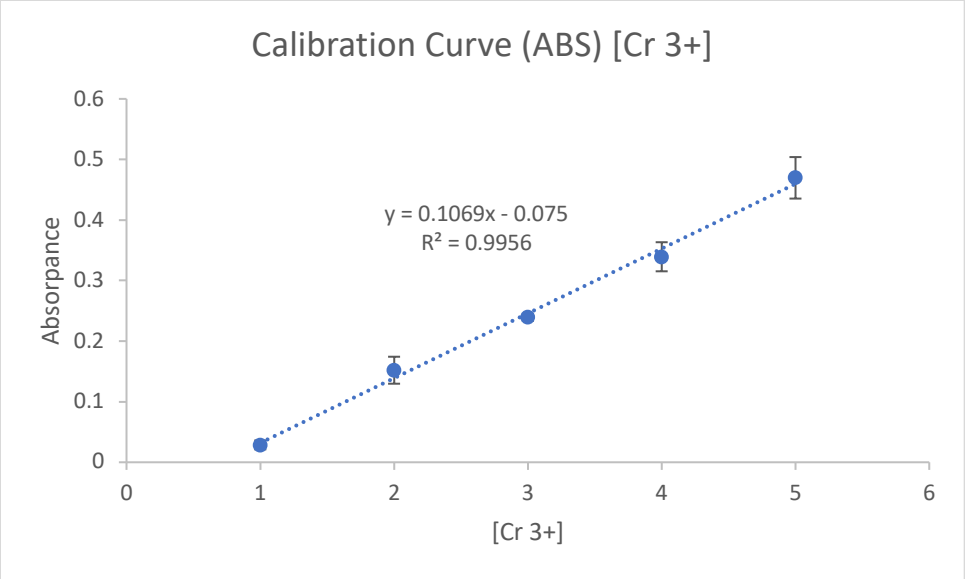

LOD 0.091627

Figure 7e. Absorbance Calibration Curve for Cr^{3+}

Solutions of 1mM dye (starting with 250 µL) and 1mM Cr^{3+} (10-50 µL) were made, diluted to 10mL with methanol (MeOH), and measured for absorbance to create a calibration curve. The limit of detection (LOD) was then calculated from the curve with the equation:

LOD= 3* SD dye/slope

to determine the lowest concentration of metal in the sample which can be detected consistently.

trial	abs	[Cr]	% recovery
1	0.209	2.65586	106%
2	0.202	2.590399	104%
3	0.192	2.496883	100%
	known	2.5	103%

Table 3a. Absorbance Accuracy Experiment for Cr^{3+}

Utilizing the calibration curve, the accuracy experiment was performed to ensure that the percent recovery for the sample was accurate (90%-110%). This was achieved by using the same solution as the calibration curve experiment, 1mM dye (250 µL) and 1mM Fe^{3+} (25 µL) and diluted with MeOH to the 10mL. Performed in triplicate to get averages and calculate the percent recovery for Cr^{3+}.

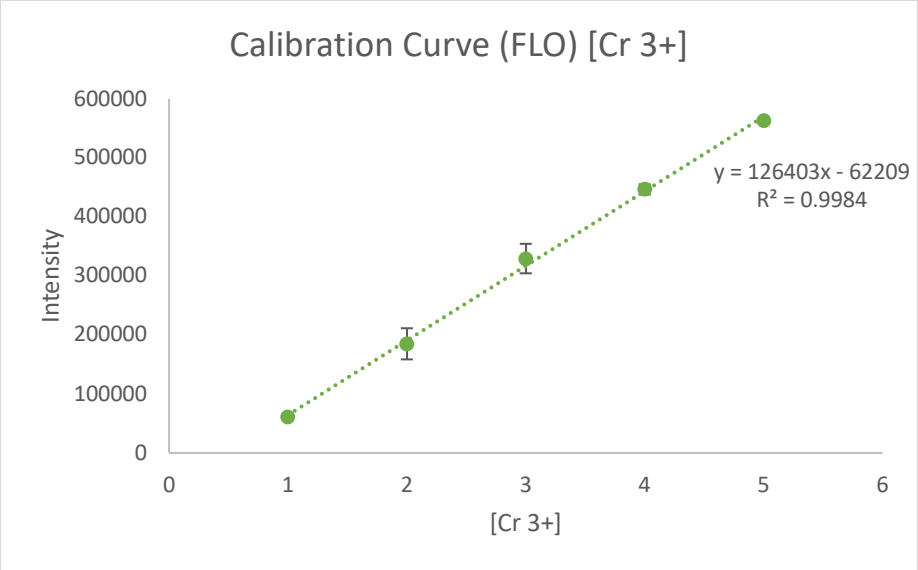

LOD 0.017686

Figure 7f. Fluorescence Calibration Curve for Cr^{3+}

Solutions of 1mM dye (starting with 250 µL) and 1mM Cr^{3+} (10-50 µL) were made, diluted to 10mL with methanol (MeOH), and measured for intensity to create a calibration curve. The limit of detection (LOD) was then calculated from the curve with the equation:

LOD= 3* SD dye/slope

to determine the lowest concentration of metal in the sample which can be detected consistently.

trial	abs	[Cr3+]	% recovery
1	270940	2.63562	105%
2	291300	2.796692	112%
3	248410	2.45738	98%
	exp	2.629897	105%
	known	2.5	

Table 3b. Intensity Accuracy Experiment for Cr^{3+}

Utilizing the calibration curve, the accuracy experiment was performed to ensure that the percent recovery for the sample was accurate (90%-110%). This was achieved by using the same solution as the calibration curve experiment, 1mM dye (250 µL) and 1mM Fe^{3+} (25 µL) and diluted with MeOH to the 10mL. Performed in triplicate to get averages and calculate the percent recovery for Cr^{3+}.

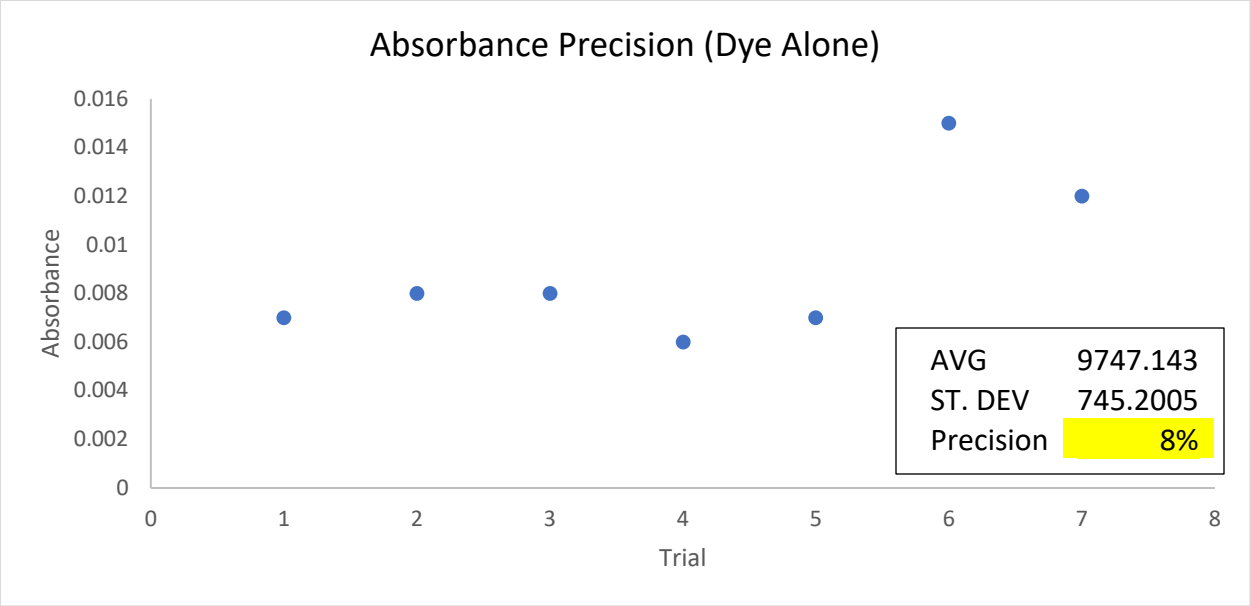

Figure 12a. Absorbance Precision Experiment for dye alone
Solutions with 1mM dye (250µL) that was diluted to 10mL with MeOH, was put in a UV viz to collect the absorbance. This was repeated 7 times to obtain the precision percentage. Precision percentage was calculated by: (AVG/ST.DEV) * 100%

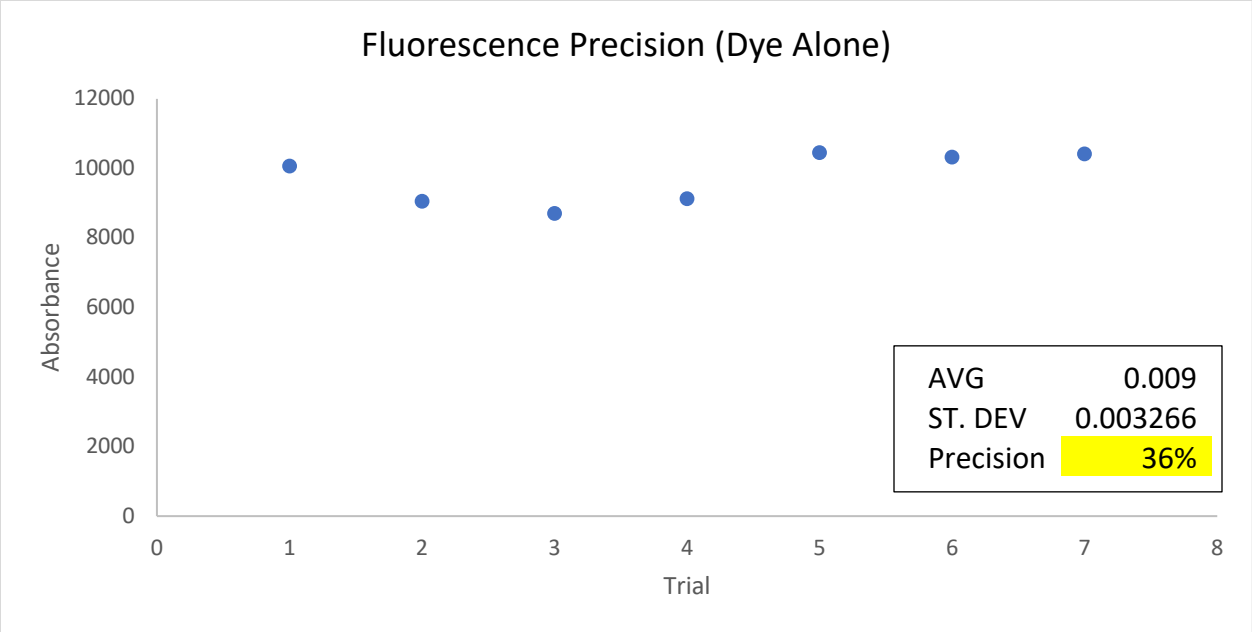

Figure 12b. Fluorescence Precision Experiment for dye alone
Solutions with 1mM dye (250µL) that was diluted to 10mL with MeOH, was put in a fluorimeter to collect the intensity. This was repeated 7 times to obtain the precision percentage. Precision percentage was calculated by: (AVG/ST.DEV) * 100%

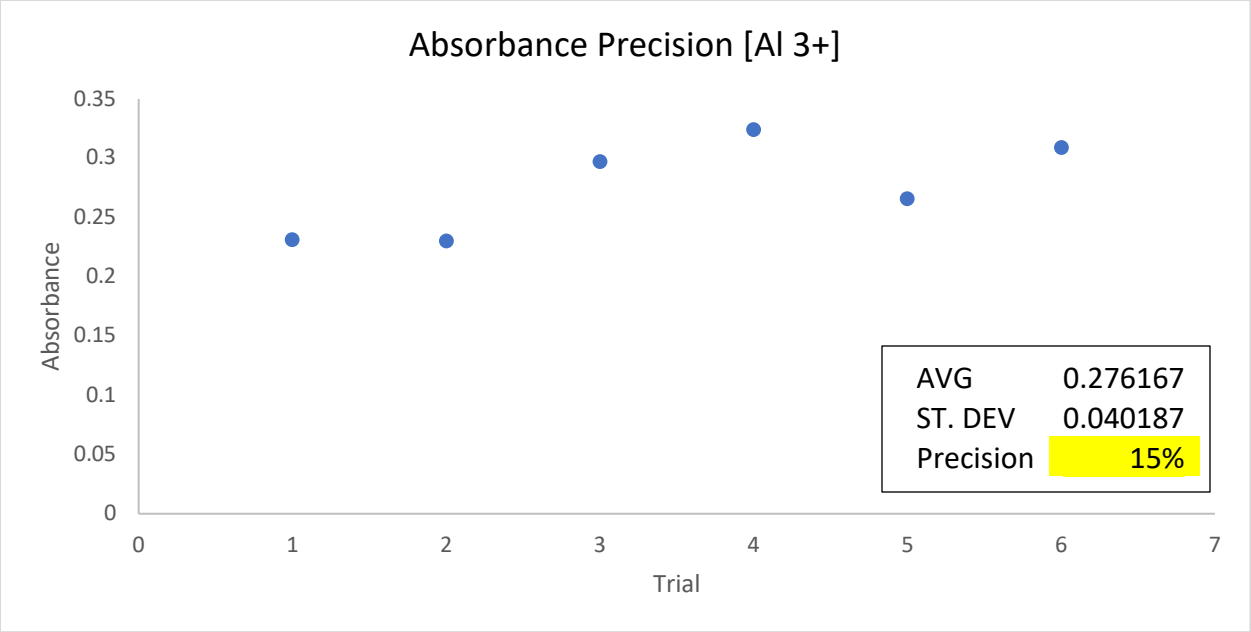

Figure 13a. Absorbance Precision Experiment for Al^{3+}
Solutions with 1mM dye (250µL) and 1mM Al^{3+}(30 µL) that was diluted to 10mL with MeOH, was put in a UV viz to collect the absorbance. This was repeated 7 times to obtain the precision percentage. Precision percentage was calculated by: (AVG/ST.DEV) * 100%

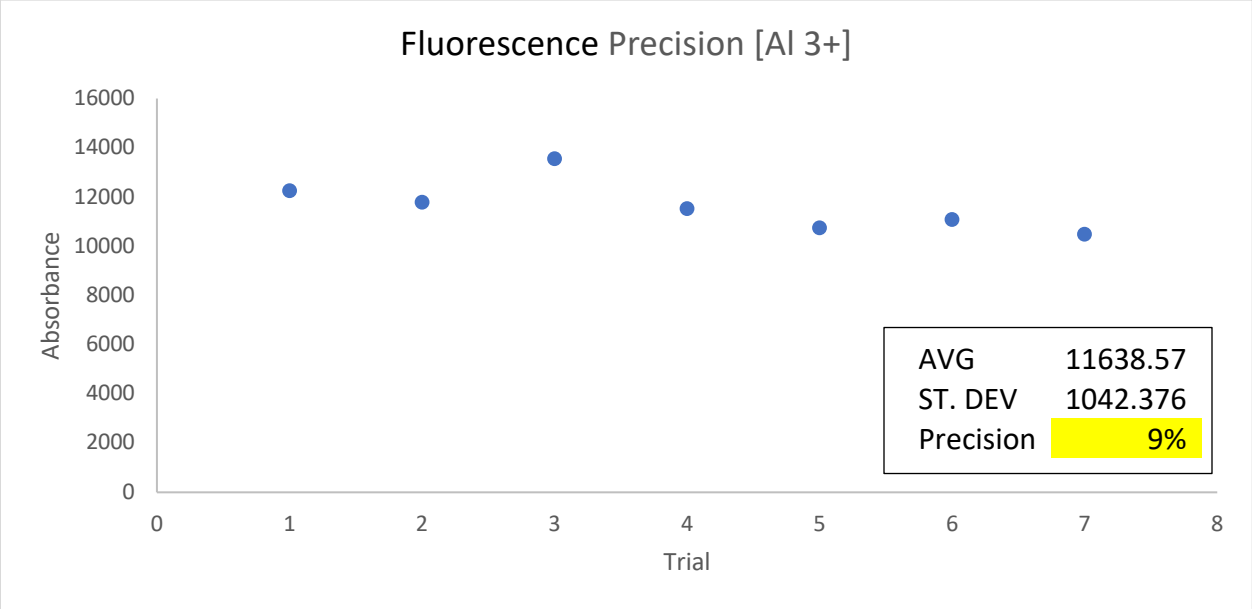

Figure 13b. Fluorescence Precision Experiment for Al^{3+}
Solutions with 1mM dye (250µL) and 1mM Al^{3+}(30 µL) that was diluted to 10mL with MeOH, was put in a fluorimeter to collect the intensity. This was repeated 7 times to obtain the precision percentage. Precision percentage was calculated by: (AVG/ST.DEV) * 100%

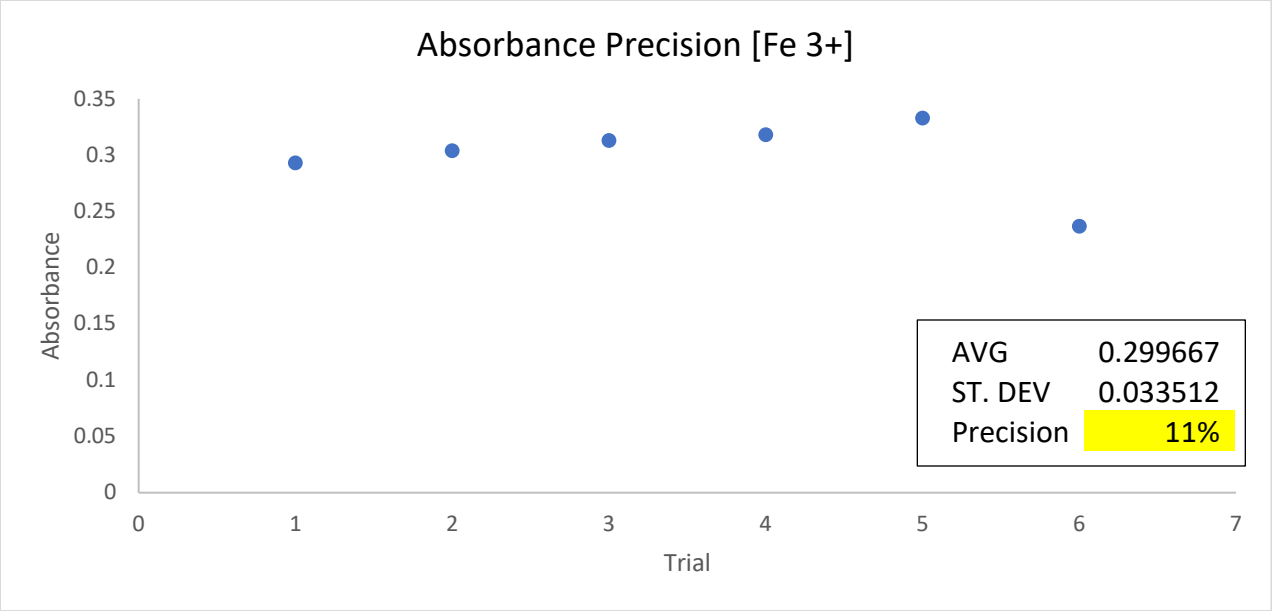

Figure 14a. Absorbance Precision Experiment for Fe^{3+}
Solutions with 1mM dye (250µL) and 1mM Fe^{3+}(30 µL) that was diluted to 10mL with MeOH, was put in a UV viz to collect the absorbance. This was repeated 7 times to obtain the precision percentage. Precision percentage was calculated by: (AVG/ST.DEV) * 100%

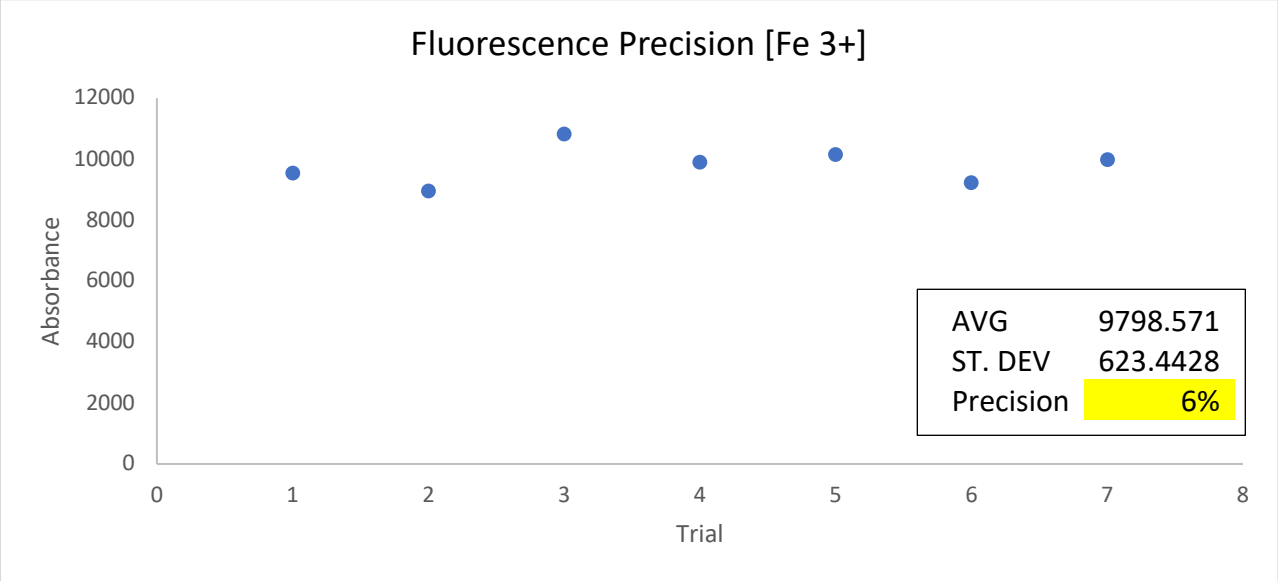

Figure 14b. Fluorescence Precision Experiment for Fe^{3+}
Solutions with 1mM dye (250µL) and 1mM Fe^{3+}(30 µL) that was diluted to 10mL with MeOH, was put in a fluorimeter to collect the intensity. This was repeated 7 times to obtain the precision percentage. Precision percentage was calculated by: (AVG/ST.DEV) * 100%

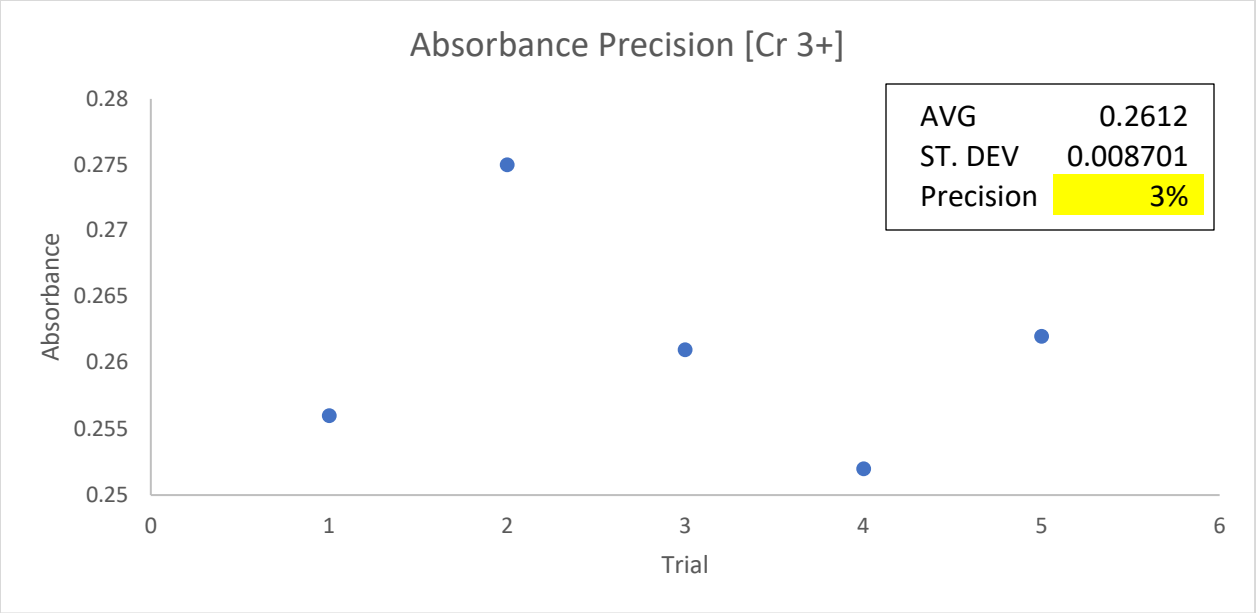

Figure 15a. Absorbance Precision Experiment for Cr^{3+}
Solutions with 1mM dye (250µL) and 1mM Cr^{3+}(30 µL) that was diluted to 10mL with MeOH, was put in a UV viz to collect the absorbance. This was repeated 7 times to obtain the precision percentage. Precision percentage was calculated by: (AVG/ST.DEV) * 100%

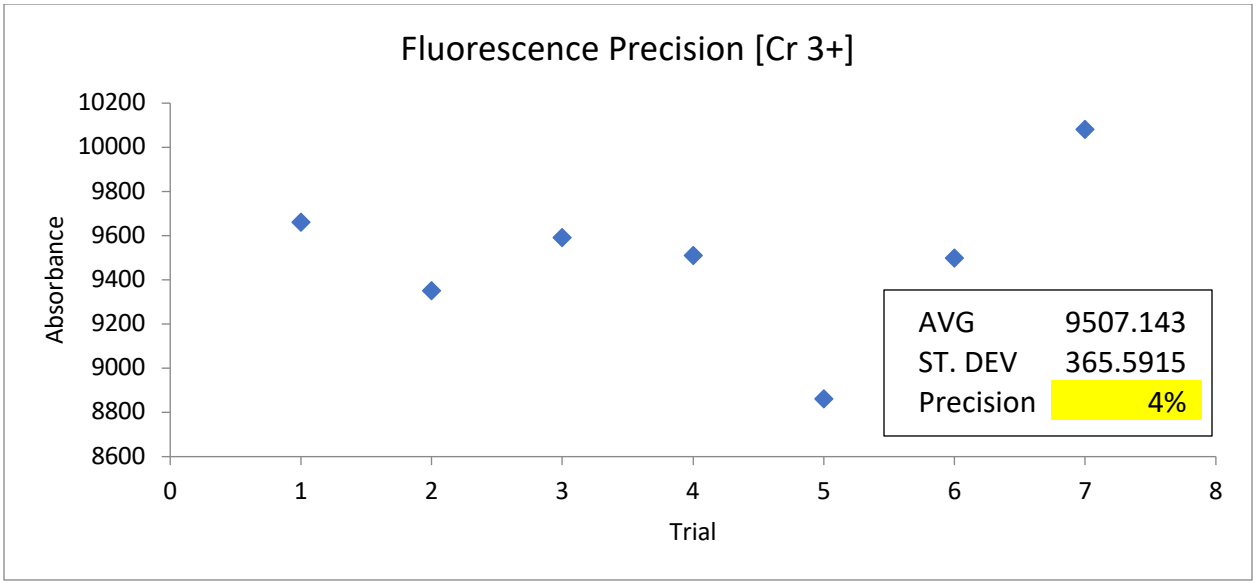

Figure 15b. Fluorescence Precision Experiment for Cr^{3+}
Solutions with 1mM dye (250µL) and 1mM Cr^{3+}(30 µL) that was diluted to 10mL with MeOH, was put in a fluorimeter to collect the intensity. This was repeated 7 times to obtain the precision percentage. Precision percentage was calculated by: (AVG/ST.DEV) * 100%